

We are IntechOpen, the world's leading publisher of Open Access books Built by scientists, for scientists

6,900

Open access books available

185,000

International authors and editors

200M

Downloads

Our authors are among the

154

Countries delivered to

TOP 1%

most cited scientists

12.2%

Contributors from top 500 universities



WEB OF SCIENCE™

Selection of our books indexed in the Book Citation Index
in Web of Science™ Core Collection (BKCI)

Interested in publishing with us?
Contact book.department@intechopen.com

Numbers displayed above are based on latest data collected.
For more information visit www.intechopen.com



Influence of Crystallization on the Properties of SnO₂ Thin Films

Daniya M. Mukhamedshina and Nurzhan B. Beisenkhanov
*Institute of Physics and Technology,
 Kazakhstan*

1. Introduction

The interest in the surface structures with their special properties has increased considerably due to extensive applications in micro- and optoelectronics. It is known that the properties of films of submicron size can be different from those of structures having macroscopic dimensions. The parameters that change the properties of films, are the thickness, number of layers, uniformity of the films, the size of clusters and nanocrystals. The presence of small particles and nano-sized elements leads to changes in material properties such as electrical conductivity, refractive index, band gap, magnetic properties, strength, and others (Suzdalev, 2006; Kobayashi, 2005).

One of the most promising materials in this regard is tin dioxide. Such advantages as high transparency in a visible range of wavelengths and high conductivity make SnO₂ very suitable as transparent conductive electrodes in such devices as solar cells, flat panel displays, etc (Rembeza et al., 2001; Jarzebski et al., 1976; Das and Banerjee, 1987; Song, 1999). Wide-gap semiconductor SnO_x films exhibit quantum confinement effect with decreasing of crystallite sizes, i.e. the band gap becomes size dependent and is increased from 3.6 to 4.2 eV.

Semiconductor gas sensors on the base of nanoscale SnO₂ films are manufactured (Evdokimov et al., 1983; Buturlin et al., 1983b; Watson et al., 1993). The possibility of tin dioxide layers to change their electrical conductivity upon adsorption of gases due to the reactions of reduction and oxidation, is used (Bakin et al., 1997; Srivastava, R. et al., 1998a; Jiang et al., 2002; Vigleb, 1989). An increase in adsorption possibilities of SnO₂ films during the transition from single-crystal to nanocrystalline system (Srivastava, R. et al., 1998b) is one of the main directions of work to improve the sensitivity and reduce of response time (Bakin et al., 1997; Ramamoorthy et al., 2003; Karapatnitski et al., 2000; Xu et al., 1991; McDonagh et al., 2002).

As is known, tin dioxide (SnO₂) is a crystal of white color, the density is 7.0096 g/cm³, melting point is about 2000°C (Knunians, 1964). The SnO₂ films have predominantly amorphous or polycrystalline structure with a tetragonal lattice of rutile with parameters $a = b = 0.4737$ nm, $c = 0.3185$ nm, with two tin atoms and four oxygen atoms in the unit cell (Dibbern et al., 1986; Shanthi et al., 1981; Weigtens et al., 1991). Depending on the method of

film synthesis, the band gap varies in the range 3.35–4.3 eV and the refractive index – in the range 1.8–2.0 (Martin et al., 1986; Melsheimer et al., 1986; Nagamoto Takao et al., 1990).

Under normal conditions in air, at the surface of tin dioxide, a layer of the adsorbed oxygen molecules is formed. Oxygen molecules carry out the electron trapping from the surface layer (Kaur et al., 2007). In the simpler schematization, in clean air the conductivity of SnO₂ is low because the conduction electrons are bound to surface oxygen, whereas in the presence of a reducing gas, electrons are no longer bound to the surface states and the conductivity increases. The transfer of electrons from SnO₂ to oxygen leads to the creation near the surface of a crystal a space charge layer (depletion layer), the concentration of electrons in which is less than in bulk. The net charge at the surface generates an electric field, which causes a bending of the energy bands in the SnO₂. A negative surface charge bends the bands upward, i.e. pushes the Fermi level into the band gap of the SnO₂, effectively reducing the charge carrier concentration and resulting in an electron depletion zone. In other words, this is an electron trapping process at the surface, which leads to an increase in the electrical resistance (or decrease in conductivity) of the surface layer. When a reducing gas, e.g. CO (or H₂, CO, H₂S, NH₃, etc.), reacts with the adsorbed oxygen to form CO₂, the concentration of oxygen in layer is decreased. The electrons released in this reaction are injected into the conduction band of the SnO₂, which results in a decrease in the electrical resistance (or increase in conductivity) of materials of n-type of conductivity (Kaur et al., 2007; Bakin et al., 1997; Andryeva et al., 1993). According to barrier model, reaction of adsorbed oxygen species with reducing gases decreases the potential barrier heights, resulting in a huge decrease in resistance.

Reduced tin dioxide is characterized by a deficiency of oxygen – SnO_{2-δ}, where $10^{-5} < \delta < 10^{-3}$ - deviation from stoichiometry (Rumyantseva et al., 2003; Kaur et al., 2007). Vacancies of ionized oxygen are the main intrinsic defects and define the electrical properties of the material – n-type of conductivity and free carrier concentration. Energy levels of oxygen vacancies V_O⁺ and V_O²⁺ lie at a depth of 30–40 and 140–150 meV below the conduction band edge, respectively (Ryabtsev et al., 2008). The concentration of oxygen vacancies can be reduced by annealing of the material in an oxygen atmosphere.

In the transition from single crystal to a polycrystalline system, each crystal grain is considered as a closed volume, near the surface of which is located a depletion layer. Reducing of the charge carrier concentration at the grain boundaries leads to a formation of intergranular energy barriers, the magnitudes of which determines the electrical conductivity of polycrystalline material as a whole. The greatest influence of the surface state on the electrical properties of the material occurs when the condition: $l/2 \leq L$, where l is the size of the crystallites; L – length of the depletion layer, which for different oxides varies

from 3 to 10 nm: $L = L_D \sqrt{\frac{eV_s^2}{kT}} = \sqrt{\frac{\epsilon kT}{2\pi e^2 N_d}} \cdot \sqrt{\frac{eV_s^2}{kT}} = \sqrt{\frac{\epsilon V_s^2}{2\pi e N_d}}$, where ϵ is the dielectric

constant, V_s – surface/Schottky potential, N_d is the concentration of the donor impurity, L_D is the Debye length, k is the Boltzmann constant, T is the temperature. Wide range of sizes of the SnO₂ crystallites (from several to several hundred nanometers) affects the mobility of charge carriers, which may vary from a few to 100 cm²/V·s. For example, Xu Chaonan et al. (1991) investigated the dependence of gas sensitivity of film on the diameter D of SnO₂ crystallites (in the range 5–32 nm) and the Debye length L_D . For undoped SnO₂ D increased

from 4 nm with increasing annealing temperature to 13 nm at 400°C and 27 nm at 900°C. The dependences of the electrical resistance of the films in air (R_a) and a mixture of hydrogen-air (R_g) at 300°C on the crystallite sizes were presented. The values of R_a and R_g increase with decreasing D for $D \leq 6$ nm, as well as increase with increasing D for $D \geq 10$ nm. The value of D at the boundary between two regions is equal to $2L$ and the optimum value for L is obtained by 3 nm. The gas sensitivity of film was determined as R_a/R_g . For the both H₂ and CO the sensitivity increases if the value $D \leq 2L$ (~ 6 nm). It follows, that the gas-sensitive properties of the tin dioxide films are determined by their nanostructure, formed during crystallization process. This makes it extremely important to study the processes of crystallization in tin dioxide films, depending on the conditions of their preparation and processing.

Good quality SnO₂ films have been grown by several techniques (Buturlin et al., 1983a). As is known, the method of preparation of SnO_x films significantly influences on their characteristics (Bakin et al., 1997; Srivastava R. et al, 1998; Jiang et al., 2002; Srivastava R. et al., 1998b; Minami et al, 1989). Not all techniques of deposition are used for production of functional metal oxide films (Buturlin et al., 1983b; Jarzebski, 1982; Khol'kin and Patrusheva, 2006). The physical methods of obtaining films of metal oxides include the method of thermal evaporation of metal in vacuum with deposition on the dielectric substrate and oxidation in air (Buturlin et al., 1983b) at 720–770K. The particles of deposited material one can obtain also by evaporation in a gas. In an atmosphere of reactive gas material is heated to evaporation, then the atoms of substance reacts with residual gas atoms, resulting in formation of ultrafine particles of size in range 1–100 nm. The resulting film has an extremely developed surface and requires no further heat treatment (Buturlin et al., 1983a). During thermal sputtering of an oxide target (Das and Banerjee, 1987; Feng et al., 1979) an annealing is not required, too. The method is based on the sputtering of target made of pressed powder of desired oxide (Jarzebski, 1982) or in plasma at high frequency in a three-electrode circuit, or by an ion beam. The spraying process is carried out in an plasma of argon of high purity with the addition of oxygen. Das and Banerjee (1987) show the relation between a structure and other physical properties of the films. For the deposited by electron-beam evaporation SnO_x films a change of x value by varying the substrate temperature T_s was revealed. The films deposited at $T_s = 150^\circ\text{C}$ were amorphous, but after annealing in air ($T_A = 550^\circ\text{C}$, 2h) the presence of SnO₂ by X-ray diffraction was revealed. Films deposited at $T_s = 225^\circ\text{C}$ were also amorphous, but after annealing under identical conditions consisted of a mixture of phases SnO and β -SnO. These amorphous films are characterized by high electrical resistivity (10^{10} ohm·cm at room temperature), which sharply decreased after annealing in air (550°C, 2 h) to the values $\rho = 9,5 \times 10^{-2}$ ohm·cm at room temperature, seemingly, due to the formation of 0.015 eV donor level ($T_s = 150^\circ\text{C}$) and 0.26 eV ($T_s = 250^\circ\text{C}$) below the bottom of the conduction band of tin oxide. For $T_s = 150^\circ\text{C}$ the band gap $E_g = 3.46$ eV corresponds to SnO₂ and decreases with increasing T_s up to 225°C due to the presence of different oxide phases, and increases again at $T_s > 225^\circ\text{C}$. Annealing in air (550°C, 2h) leads to deterioration of the transmission T in the wavelength range of 400–850 nm for the films deposited at $T_s = 150^\circ\text{C}$ and to the increase of transmission for films deposited at $T_s \geq 250^\circ\text{C}$. At $T_A = 650^\circ\text{C}$ the full transformation into the SnO₂ phase with the dominant lines (101) and (200) is completed. The increase of the substrate temperature ($T_s = 350^\circ\text{C}$) causes a decrease in the resistance of the film, indicating that activation occurred because of donors at a depth of 0.26 eV.

In the method of ion-stimulated deposition (Song, 1999) flow of neutral Sn atoms was obtained in a high vacuum using partially ionizing radiation source, the flow of oxygen ions with energies in the range 0-1000 eV was obtained using ion gun with hollow cathode. The properties of SnO₂ films on substrates of glass, amorphous SiO₂/Si and Si (100) were studied. In films deposited on glass, with increasing of the energy of the ion flux both the surface grain size up to 7–10 nm and roughness are increased. The increase of energy of the oxygen ions led to the increase of crystal perfectness, stoichiometry, porosity of the films and their transmission in the shortwave region. All tin oxide films on the glass after deposition had very low optical absorption in the visible wavelength region and high absorption in the shortwave region.

Method for production of SnO₂ films by cathode sputtering of tin provides the creation of plasma in an inert gas (argon) at a pressure in the vacuum chamber from 50 to 10⁻² Pa. A target is fixed to the cathode, substrate – to the anode. When the diode sputtering is used, between the anode and cathode DC voltage is applied, the growth rate of SnO₂ films is small (~ 1.7 nm/min) and only conductive targets can be used. In the high-frequency sputtering, between the cathode and the anode an alternating RF voltage is applied. As a result, high-speed deposition of the layer up to 800 nm/min is provided, depending on the voltage and the partial pressure of O₂ and Ar. One can use a non-conductive target. Conductivity of SnO₂ films varies in the range 10⁻⁹–10² ohm⁻¹·cm⁻¹.

One of the most promising physical methods of production of the oxide films is the reactive magnetron sputtering of a metal target (Geoffroy et al., 1991; Kisin et al., 1999; Lewin et al., 1986; Semancik and Cavicchi, 1991). As a result of the deposition process, a mixture of two phases - SnO and SnO₂ - is formed. By changing the parameters of deposition (substrate temperature, chamber pressure, the rate of film growth) both amorphous and nanocrystalline films can be prepared. For example, Semancik S. and Cavicchi R.E. (1991) by this method have deposited the SnO₂ films on substrates of sapphire and TiO₂. It is shown that the use of substrates with perfect structure and an increase in their temperature up to 500°C leads to the epitaxial growth of the film and the formation of a single crystal structure. Gas sensitivity of the films was close to sensors based on bulk single-crystal SnO₂. Using a VUP-4 installation, Rembeza et al. (2001) have deposited polycrystalline SnO₂ films with thickness of 1–5 microns on glass substrate by magnetron sputtering of tin target doped by antimony (3% vol.) in a gas mixture of Ar (25%) and O₂ (75%). In the films has been revealed only a well-crystallized tetragonal phase of SnO₂ with average grain size 11–19 nm after annealing. After annealing of the films (600°C, 4h) the concentration of electrons decreases with the increase of temperature up to 400°C in the range ~ 2×10¹⁸ – 3×10¹⁷ cm⁻³, and the mobility of free charge carriers increases from 70 to 150 cm²/(V·s) at 130°C and further up to 400°C does not change. Stjerna and Granqvist (1990) studied the optical and electrical properties of SnO_x films, obtained by magnetron sputtering of tin in a mixture of argon and oxygen. The optical properties show a transparency window in the wavelength range of ~ 0.4–2 microns. It is noted that the behaviors of the curves of transmission and reflection strongly depend on the ratio of values of partial pressure of O₂ and Ar during the growth of the films, and is particularly strong changed near ratio of ~ 4%. Near this point (from 4.1 to 4.2% vol. O₂) a sharp minimum of the surface resistance is observed. If the power discharge is increased from 10 to 60 watts, the position of minimum is shifted toward higher concentrations of oxygen – up to 11.6–11.8%. Kisin et al. (2000) gave a description of

dependence of the concentration of free electrons on the partial pressure of oxygen for the film deposited by rf magnetron sputtering of target, prepared from powder of SnO₂ doped with CuO, followed by a two-hour annealing in a flowing oxygen at a temperature of 700°C. Polycrystalline SnO₂ films with an average grain size of 100 nm and a thickness of 1 micron were monophasic and had a texture in the (110). In the range of partial pressure of oxygen in the chamber from 0.013 to 1.3 Pa a power dependence of the conductivity of the films on the pressure with an exponent of 0.6–0.8 is observed. Rumyantseva et al. (2001) showed that the effect of porosity on gas sensitivity of the film is more significant than the influence of the partial pressure of oxygen. Saturation by vacancies and the formation of pores in the gas-sensitive layers was carried out by doping the initial loading of tin by volatile impurities - iodine and tellurium. The porosity of the material with a grain size comparable with the wavelength of the radiation manifests itself in the form of reducing the magnitude of the refractive index, averaged over the volume.

Chemical methods of preparation of SnO₂ films can be divided as obtained from the gas phase and from solution. Hydrolysis of chemical compounds in the gas phase occurs at relatively low temperatures. The chlorides and other compounds easily hydrolyzed in the vapor phase and are deposited as thin films of hydroxides (Suikovskaya, 1971). Obtaining of the corresponding oxides is carried out by annealing or by deposition on the heated substrate. Depending on the temperature of the substrate, the amorphous or polycrystalline films can be produced (Melsheimer and Teshe, 1986). In chemical vapor deposition (Kern and Ban, 1978), the laminar flow of an inert carrier gas completely covers the substrate in the reaction chamber, forming over it motionless boundary layer. The reagents are fed as a vapor-gas mixture, the deposition rate of which depends on the speed of their diffusion through the boundary layer. Growth of the SnO₂ films (Kim and Chun, 1986) can occur in several modes. The optimal regime is the nucleation on the substrate surface and their growth by surface diffusion of the incoming material. This leads to the texturing of the film due to the formation of oriented nuclei on the surface.

To obtain homogeneous films of SnO₂ from solutions one must take into account the properties of precursors and solvents. As a precursor the tin chlorides are often used. Suitable solvents include ethanol and acetone containing a small amount of water (Suikovskaya, 1971). Aerosol methods of producing of tin oxide films are based on the decomposition at high temperature (720–970 K) of chloride or organometallic tin compounds on the surface of the substrate. At spraying under the influence of the inert gas, the solution was transferred to the substrate surface in the form of small droplets. The deposition rate of films is 100 nm/min. Dimitrov et.al. (1999) by the hydrothermal method ($t_{\text{sint}} = 130\text{--}250^\circ\text{C}$, $\tau_{\text{sint}} = 2\text{--}6\text{ h}$) synthesized nanocrystalline samples of SnO₂. Crystallite size of SnO₂, synthesized by hydrothermal treatment of amorphous gel of tin acid is 4–5 nm and is virtually independent of temperature and duration of treatment.

An actively developing chemical method of producing of SnO₂ thin films is a sol-gel method. It is based on transfer of a substance in the sol and gel states. The method allows obtaining the multilayer films with a thickness of one layer of 2–3 nm, and it does not require a vacuum and complex installations. Deposition of the film can occur on a cold substrate. The main methods of film deposition are dip-coating, centrifugation (spin-on-films) and spray pyrolysis (Kim and Chun, 1986; Aranowich et al., 1979; Sanz Maudes and

Rodriguez, 1980; Fantini and Torriani, 1986; Jitianu et al., 2003; Chatelon et al., 1997). It is one of the simplest and economic among known techniques. The advantages of the sol-gel process are the possibility of doping and its potential to fabricate films of large area substrates. The flexibility of the technological cycle management provides opportunities to obtain the necessary surface morphology and sizes of structural formations. One can obtain the films with a high degree of homogeneity and controlled stoichiometry by sol-gel method at a sufficiently low temperature of synthesis. Often (Suykovskaya NV, 1971; Zang and Liu, 1999) salt volatile acids, such as chlorides, as film-forming substances are used. As a solvent mainly ethanol is used. Chlorine can be included in the formed SnO_2 film or by replacing the oxygen, or by interstitial mechanism (Bosnell and Waghorne, 1973; Aboaf et al., 1973). The admixture of chlorine causes an increase in carrier concentration, leads to the stabilization of the parameters of the oxide layer, to a low density of surface states, and to high values of the lifetime of the major carriers. Growth of SnO_2 crystallite size after annealing is noted by many authors (Asakuma et al., 2003; Brito et al., 1997). However, the introduction of additional components in the composition of the film-forming mixture (Torkhov et al., 2003) leads to a decrease in the rate of growth of crystallites of the both SnO_2 and substance injected with increasing temperature. Torkhov et al. (2003) synthesized the nanocrystalline SnO_2 and WO_3 and nanocomposite $\text{Sn}:\text{W} = 1:9, 1:1, 9:1$ by $\alpha\text{-SnO}_2 \cdot n \cdot \text{H}_2\text{O}$ and $\text{WO}_3 \cdot \text{H}_2\text{O}$ (series X) gel deposition and kristol-method (series K). For nanocomposites of Sn (X, K) and Sn_9W_1 (X, K) after annealing at $T \geq 150^\circ\text{C}$ a phase of tin dioxide SnO_2 (cassiterite) was detected, the degree of crystallinity of which increases with increasing temperature. An increase in the crystallite size of SnO_2 (2–15 nm) and WO_3 (10–50 nm) is also observed. For SnO_2 films the change of grain size in range from 10 to 6 nm is accompanied by increase of resistance from 2×10^4 up to 6×10^4 ohms. Anishchik et al. (1995) annealed the films obtained by centrifugation from an aqueous solution at temperatures of 400 or 500°C for 30 minutes with further rapid cooling in air ("hardening of soft"). In SnO_2 films, subjected to cooling from 400°C , the SnO phase also found. Rapid cooling from 500°C leads to an appearance of Sn_3O_4 phase, while at slow cooling this phase is not detected. Rapid cooling of the samples from temperatures of 400 and 500°C leads to "freezing" on the surface of films of elemental tin and its oxides, as they do not have time to oxidize up to SnO_2 .

The films to ensure maximum sensitivity are heated during operation of sensors. The temperature effect causes an increase in the crystallite sizes of SnO_2 . On the one hand, there is a reduction of the effective activation energy of the interaction of SnO_2 with oxygen, and, on the other hand, increasing the concentration of electrons with sufficient energy to overcome the barrier created by the negatively charged surface (Rumyantseva et al., 2008). The degree of surface coverage by chemisorbed oxygen $\text{O}_{(\text{ads})}^-$, $\text{O}_{(\text{ads})}^{2-}$ is increased. The films with a fixed size of the crystallites SnO_2 are required to ensure a long-term operation of the sensors. Kukuev and Popov (1989) used a SnO_2 film in the manufacture of microelectronics devices in installations for heating of ultrapure deionized water, as well as in commercially available installations for infrared heat treatment of photo resist as heating elements. The most suitable as heaters are the films with grain size $\sim 0.2\text{--}0.3 \mu\text{m}$, in which such processes as crystallization, condensation and oxidation do not occur. Adamyan et.al. (2006) obtained high-quality films using sodium stannate as a precursor. 1 M of H_3PO_4 was added into Na_2SnO_3 solution with constant stirring to neutralize the solution ($\text{pH} = 7$). The transparent, stable sol, indicating the small size of its particles and the stability of their surface, was obtained.

One of the ways to improve the selectivity of sensors based on SnO₂ and increase the contribution of molecules of this type in the gas phase to the total electrical signal is the introduction of alloying elements into highly dispersed oxide matrix (Rumyantseva et al., 2003; Fantini and Torriani, 1986; Okunara et al., 1983 ; Bestaev et al., 1998). Dopants are usually divided into two groups: catalytic (Pt, Pb, Ru, Rh) and electroactive (In, Sb, Cu, Ni, Mn). Of considerable interest is also the effect of processing by plasma on the properties of films. Minami et al. (1989) placed the transparent conductive films of tin oxide (TCO) in a quartz tube filled with hydrogen gas. Films at high temperature treatment are completely painted in dark gray. Transmittance of ITO indium doped and undoped TO films decreased rapidly during annealing above 300°C for 30 minutes. Decrease the transparency and color of the films are attributed to the formation of the oxygen-depleted surface level due to chemical reduction of these films by hydrogen. The upper surface of the films passed into the metallic state, and then indium and tin were thermally evaporated at a higher temperature. Hydrogen glow discharge plasma was obtained at a pressure of 400 Pa in the installation with a capacitive circuit (frequency of 13.56 MHz or 2.45 GHz) and power of 300 watts. Transmittance and film thickness are greatly reduced when exposed by hydrogen plasma at 250°C. ECR hydrogen plasma was obtained in the volumetric resonator cavity at a pressure of 6.5×10^{-2} Pa, microwave power (2.45 GHz) 300 watts when a magnetic field was 8.75×10^{-2} T. Indium containing (ITO) film and undoped (TO) SnO₂ were stained even when treated for 2 and 5 minutes.

An analysis of published data shows that in papers a great attention is paid to influence of the structure of the synthesized tin dioxide films on their sensitivity to different gases and transparency in a wide range of wavelengths. Usage of different methods of preparation, as well as modification of the films by different types of treatments leads to a change of phase composition and microstructure of the films causing a change in their optical, electrical and gas-sensitive properties. It is of considerable interest to study the effect of the concentration component, nanoclusters, the composition of films and their heat or plasma treatment on the crystallization processes and clustering, the size of the nanocrystals and, consequently, the physical properties of the films.

In this paper we consider the influence of composition and structure on the optical and electric characteristics of SnO_x thin films deposited on glass substrates by sol-gel technique. For comparison, the data for films prepared by magnetron sputtering, are presented. Using various techniques the effect of both thermal and plasma treatments on the structure and properties of the SnO_x films were studied.

2. Experimental

A solution to obtain the nanostructured films by sol-gel technique (the method of spreading) was prepared from crystalline hydrate of tin tetrachloride (SnCl₄·5H₂O) by dissolution in pure ethanol. SnO₂ sol of desired concentration was obtained under strong stirring to obtain a colorless and transparent solution. Freshly prepared solution has a neutral pH value of ~ 7. After maturation of the solution, which lasted more than six hours, pH was equal about 0.88, indicating the release of HCl during the dissolution of SnCl₄. To study the effect of concentration of components in the solution on the film properties were obtained the solutions with a concentration of tin atoms: 0.82, 0.41, 0.30 and 0.14 mol/L. Aliquots of these solutions with volumes of 0.04 ml, 0.08 ml, 0.11 ml, 0.23 ml, respectively, using

micropipettes were deposited on the cleaned surface of the microscope glass slides. It was assumed that the number of tin atoms in the films will be identical ($\sim 3.25 \times 10^{-5}$ mole), and the film thickness is ~ 350 nm. After the deposition, the films were dried for 1 hour at 80°C . Then the samples were annealed at 100, 200 or 400°C for 1 hour. The thickness of the films, estimated from the change in mass of the sample, was 360 ± 40 nm.

The SnO_2 films with thickness of 300 nm were also fabricated by method of centrifugation. A solution was obtained by dissolving of anhydrous SnCl_4 in 97% ethanol. The solution was deposited onto a glass substrate located on a table of centrifuge rotor, the rotation speed of which was ~ 3800 rpm. Centrifugation time was 3–5 s. Substrate with a layer was dried using an infrared radiation at 80°C for 3–5 minutes, and then in a muffle furnace at 400°C for 15 minutes. After cooling, the cycle repeats. Number of deposited SnO_2 layers ranged from 12 to 15.

The SnO_2 films with thickness of 300 nm were also deposited on cleaned microscopy glass slides by magnetron sputtering. The magnetron sputtering mode parameters were: cathode voltage $U_c = 470$ V, the ion beam current $I_{\text{ion}} = 35$ mA, the argon-oxygen mixture pressure inside the chamber $\sim 1\text{--}2.7$ Pa, the oxygen concentration in the Ar- O_2 mixture $\sim 10\%$, deposition rate of films ~ 0.05 nm/c, the temperature of the substrate $\sim 200^\circ\text{C}$.

The SnO_2 film's structure was investigated by X-ray diffraction using a narrow collimated (0.05×1.5 mm²) monochromatic (CuK_α) X-ray beam directed at an angle of 5° to the sample surface. The average crystallite size was estimated from the width of X-rays lines by Jones method. The surface of the layers was analyzed by Atomic force microscopy (JSPM 5200, Jeol, Japan) using AFM AC technique. The optical transmittance spectra of SnO_x films were measured in the wavelength range from 190 to 1100 nm by means of the SF-256 UVI and from 1100 to 2500 nm by means of the SF-256 NIR spectrophotometers (LOMO, Russia). Electrical resistance of the films was measured by a four probe technique at room temperature. For the measurements of electrical characteristics and parameters of gas sensitivity of the thin films in a wide temperature range was used a specialized experimental setup.

The glow discharge hydrogen plasma was generated at a pressure of 6.5 Pa with a capacitive coupled radio frequency (r.f.) power (27.12 MHz) of about 12.5 W. The temperature of processing did not exceed 100°C . The processing time was 5 min.

3. Results and discussion

3.1 Physical properties of tin oxide thin films obtained by sol-gel technique (the method of spreading)

Fig. 1 shows the transmission spectra of SnO_x films deposited on a glass substrate by spreading method. Transparency of films lies in the range of 80-90% and increases over the entire range of wavelengths with the increase of temperature up to 400°C .

X-ray diffraction studies of the SnO_x films, obtained at various concentrations of tin ions in the colloidal solutions, led to the following results.

- a. In the case of high tin concentration 0.83 mol/L (~ 0.04 ml aliquot) immediately after deposition and drying at 80°C , the film structure is similar to the amorphous (Fig. 2a)

and remains practically unchanged after annealing for 1 hour at 100°C (Fig. 2b). Separation of the broad band into two SnO₂ lines, indicating the formation of crystallites, visually observed only after annealing at 200°C (Fig. 2c). Crystallite size in the planes (110) and (101) of SnO₂ is ~ 1.5 nm, i.e. the crystallites are small and have an imperfect structure.

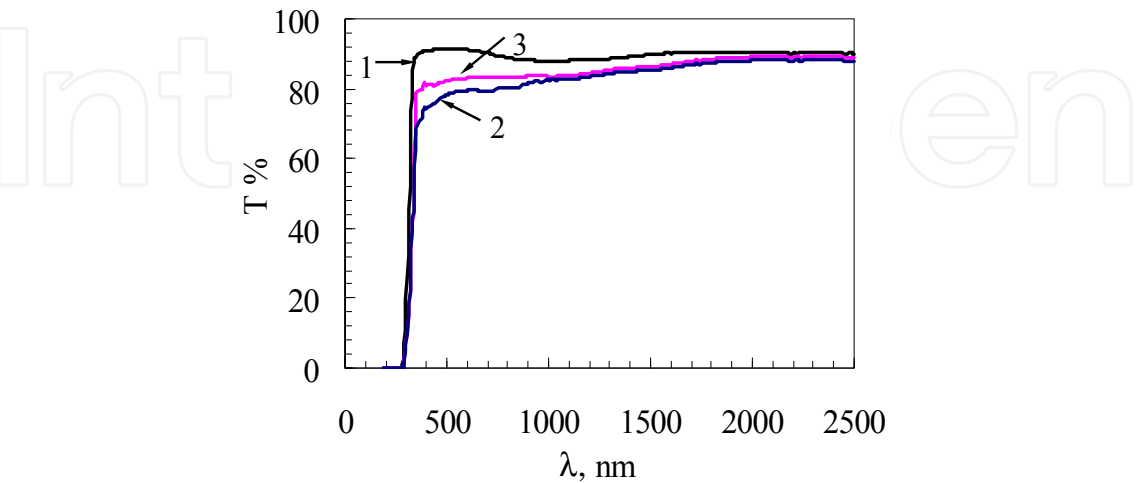


Fig. 1. The transmission spectra of tin oxide film synthesized by sol-gel technique: 1 – glass substrate, 2 – SnO₂ film after annealing at 100°C, 3 – SnO₂ film after annealing at 400°C.

- b. A similar pattern after the deposition and annealing at 100°C is observed for films of SnO₂, produced at lower tin concentrations of 0.41 mol/L (~ 0.08 ml aliquot) and 0.30 mol/L (~ 0.11 ml aliquot). After annealing at 200°C the differences are appeared, which manifest themselves in increasing intensities of SnO₂ lines with decreasing of tin concentration in the colloidal solution.

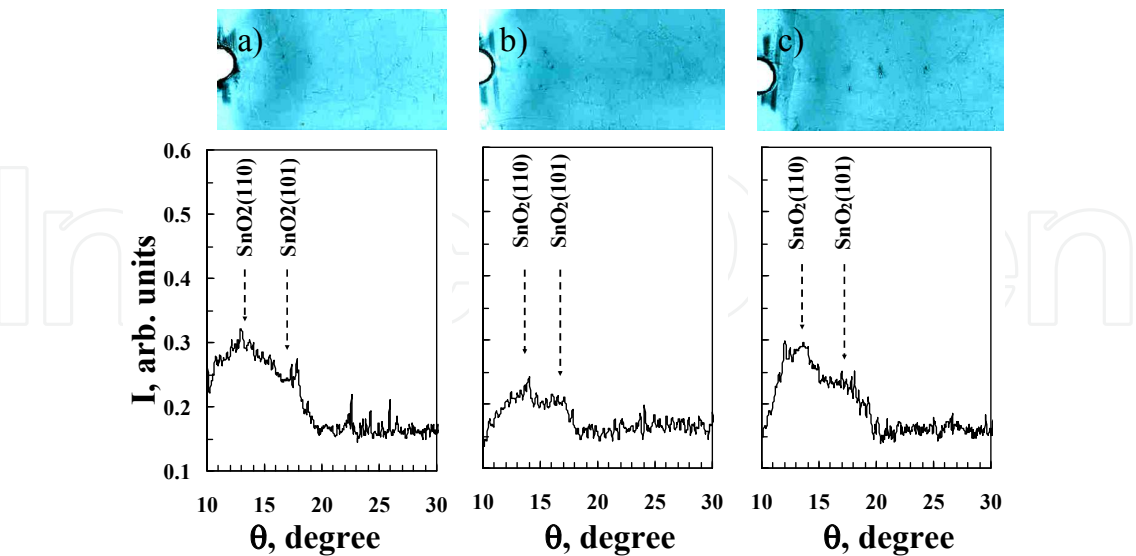


Fig. 2. X-ray diffraction patterns and intensity curves for the SnO_x films on glass substrates obtained by the sol-gel technique (0.04 ml solution with tin concentration of 0.83 mol/L, d = 320 nm) after: a) deposition and drying at a temperature of 80°C, and b) annealing at 100°C; c) annealing at 200°C.

- c. In case of the minimum concentration of 0.14 mol/L (~ 0.23 ml aliquot), the formation of a SnO₂ polycrystalline film (Fig. 3a) with a crystallite size of 2.5–3.5 nm (Table 1) was observed immediately after deposition and drying. Annealing at 400°C led to the improvement of the crystallite perfection (4 lines) and an increase in their size up to ~ 5 nm (Fig. 3b).

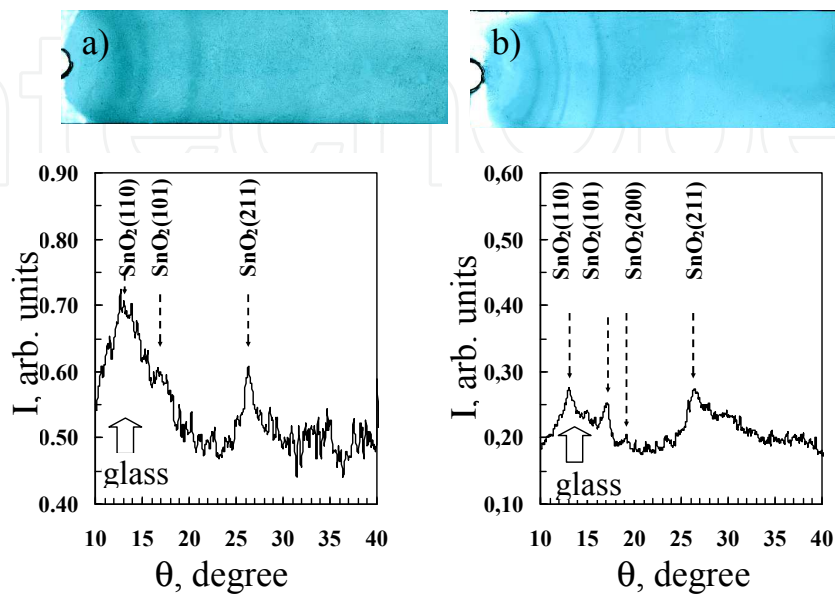


Fig. 3. X-ray diffraction patterns and intensity curves for thin SnO_x films on glass substrates obtained by the sol-gel technique (0.23 ml solution with tin concentration of 0.14 mol/L, d = 400 nm): a) after deposition and drying at a temperature of 100°C, b) after annealing at 400°C.

SnO ₂ plane	Crystallite size after annealing, nm	
	100°C	400°C
SnO ₂ (110)	2.5	5.5
SnO ₂ (101)	3.0	5.0
SnO ₂ (211)	3.5	3.0

Table 1. Results of measurements of SnO₂ crystallite sizes by X-ray diffraction

Thus, the SnO₂ polycrystalline film immediately after deposition and drying without additional annealing at elevated temperatures by the sol-gel technique was derived. This may be due to better conditions for the processes of SnO₂ crystallization and evaporation of HCl in the case of a lower concentration of tin atoms (0.14 mol/L) in solution. Additional annealing at 400°C leads to the formation of SnO₂ crystallite with size of about 5 nm, ie close to optimal (6 nm) for high gas-sensitive films (Xu et al., 1991).

Gas sensitivity was determined from the expression $\gamma = \frac{R_0 - R_g}{R_0} \cdot 100\% = \frac{\Delta R}{R_0} \cdot 100\%$, where

R₀ is the resistance of gas-sensitive layer in the clean air, R_g is the resistance of the layer in the mixture of air with detectable reducing gas. Fig.4 shows the temperature dependence of the sensitivity of SnO₂ film for a given concentration of ethanol vapor in the atmosphere. Since the temperature range of sensitivity to different gases is different, it is

necessary to determine the temperature at which a maximum sensitivity of the film to the test gas is observed.

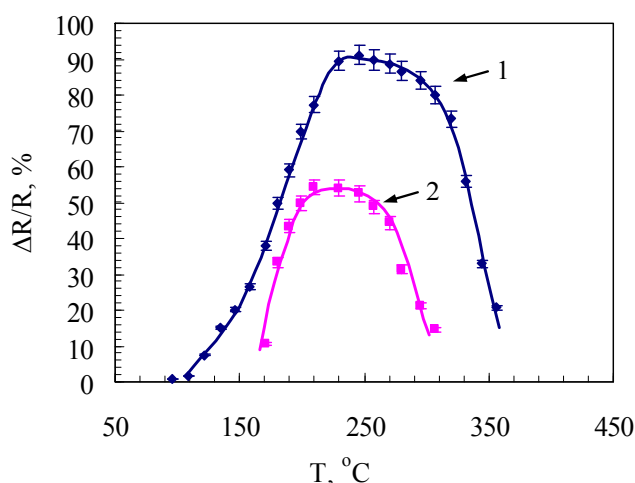


Fig. 4. Temperature dependence of the sensitivity of the SnO₂ films (obtained from a colloidal solution with concentration of tin ions 0.14 mol/L) to the ethanol vapors of various concentration: 1 – 15 mg/L of ethanol in the air; 2 – 0.7 mg/L of ethanol in the air.

The greatest sensitivity of films to ethanol is observed at a temperature of 230°C. Adsorbed oxygen ions create a space charge region near the surface of SnO₂ grains by extracting electrons from the material. Ethanol, being by nature a reducing gas, reacts with adsorbed O⁻ ions and removes them from the surface of the grains, re-injecting electrons back into the material and thus lowering the resistance of the film. Peak sensitivity at 230°C shows that at this temperature, the amount of chemisorbed oxygen ions, which react with the molecules of ethanol, is maximal.

In Fig. 5 the sensitivity of the SnO₂ films at 230°C as a function of the concentration of ethanol vapor is presented. Figs. 4 and 5 show that sensitivity increases significantly with increasing of ethanol concentration. At low concentrations of ethanol vapor (0.1–1 mg/L), the dependence of the film sensitivity on the concentration is linear (Fig. 5), as is likely, there is a sufficient number of oxygen ions that react with molecules of ethanol. Linearity of sensitivity at low concentrations of ethanol can be used to create sensors basing on this film, which are sensitive to ethanol vapor in exhaled human. A visible sensitivity of the film is evident even when the concentration of ethanol vapor is about 0.05 mg/L (25 ppm).

The films obtained by deposition of a colloidal solution with a concentration of tin atoms 0.83 mol/L (Fig. 5, curve 1), have higher gas sensitivity in comparison with films deposited from a solution with a concentration of tin atoms 0.14 mol/L (Fig. 5, curve 4). This may be due to the cluster structure of the film synthesized from a solution with a concentration of tin atoms 0.83 mol/L. Indeed, the average size of the crystallites in these films is much smaller (1.5 nm).

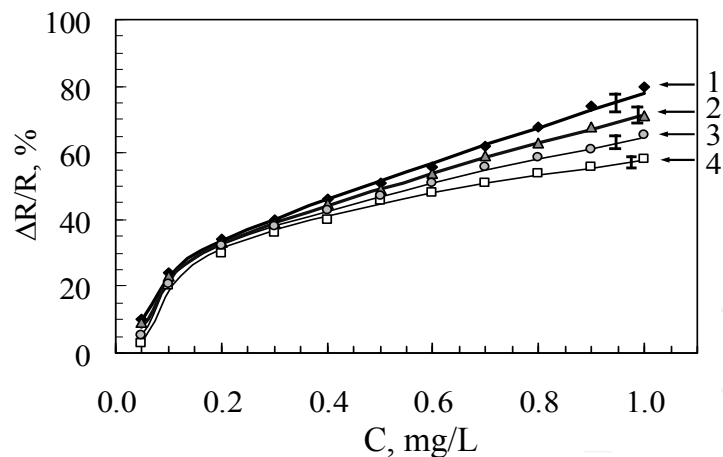


Fig. 5. The dependence of the sensitivity of the SnO₂ films on the concentration of ethanol vapor at 230°C: 1 – film synthesized from a solution with a concentration of tin ions 0.83 mol/L, 2 – 0.41 mol/L, 3 – 0.30 mol/L; 4 – 0.14 mol/L.

To measure the response time, the changes of resistance are recorded as a function of time beginning from the moment when ethanol vapors are introduced into the chamber. The concentration of ethanol wondered equal to 1 mg/L (500 ppm) at $T = 230^{\circ}\text{C}$. As a response time of the sensor was taken the time duration for which the sensor resistance dropped by 90%. Response time and recovery time of resistance to the initial value for the film deposited from a colloidal solution with a concentration of tin atoms 0.83 mol/L (Fig. 6, curve 1) are ~ 3 and 30 seconds, respectively, in contrast to the second film (0.14 mol/L), where response time and recovery time were twice as much – ~ 6 and 65 seconds, respectively.

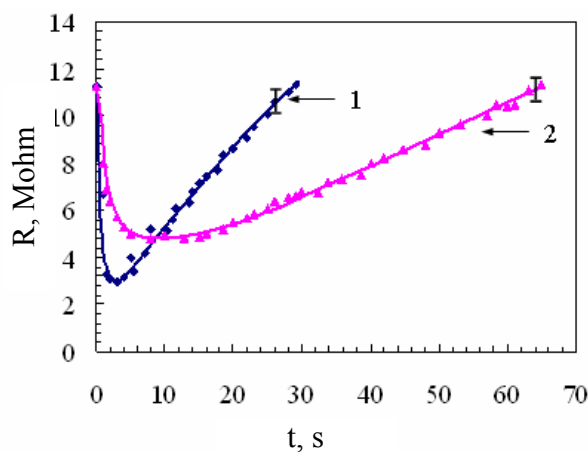


Fig. 6. The dependence of the response time of SnO₂ layer at 230°C (concentration of ethanol vapors 1 mg/L) on concentration of tin atoms in colloidal solution: 1 - 0.83 mol/L, 2 - 0.14 mol/L.

Figs 7a and 7b show the atomic force microscopy and scanning electron microscopy images, respectively, of the surface of tin oxide film, obtained by deposition of a colloidal solution with a tin concentration 0.83 mol/L on a glass substrate. Areas, protruding above the surface, have a light color, areas below the surface have a dark color (Fig.7a), and counting the height begins from the bottom point. In the process of drying, the SnO₂ film, obtained by

the method of spreading, is transformed into a structure with an undulating surface, the wave amplitude of which is comparable to the thickness of the film. The heterogeneity of the thickness of the films may be the main reason for the lack of interference in the transmission spectra. Consequently, in order to obtain uniform thickness of the films with relatively smooth surface the centrifugation method was used, when under the centrifugal force during the sample rotation the alignment of the surface is reached.

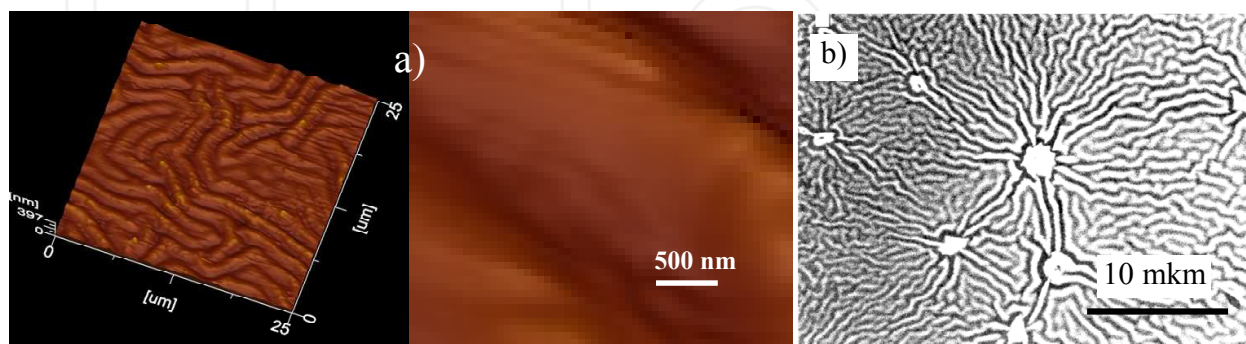


Fig. 7. Surface topography of tin dioxide film synthesized by sol-gel technique (a method of spreading, a colloidal solution with a tin concentration 0.83 mol/L): a) atomic force microscopy; b) scanning electron microscopy

3.2 Optical, electrical, structural and sensory properties of the SnO_x films, prepared by the sol-gel technique (centrifugation method)

The films were made by centrifugation in order to reduce their electrical resistance. Scheme of the synthesis and study of the SnO₂ films is shown in Figure 8. A solution of the desired tin concentration for producing of SnO₂ film with thickness ~ 300 nm was obtained by dissolving of anhydrous SnCl₄ in 97% ethanol. Kinematic viscosity of the solution was ~ 1.9 mm²/s. The radius of sol particles in solution, determined by the turbidimetric method

according to formula $r = \sqrt[3]{\frac{3V}{4\pi}}$, was 5.4 nm. The solution was deposited on a glass substrate,

located on a table of centrifuge rotor. Rotational speed of the centrifuge was ~ 3800 rpm. Centrifugation time was 3–5 seconds. The deposited films were dried by an infrared emitter at 80°C for 3–5 minutes and also in a muffle furnace at 400°C for 15 minutes.

As shown above, the films obtained by spreading, in the case of high concentration of tin atoms (0.83 mol/L) had higher gas sensitivity and lower response time and recovery time compared to films with a low concentration of tin atoms (0.14 mol/L). However, the films obtained by centrifugation from solution with a high concentration of tin atoms (0.83 mol/L) were susceptible to detachment due to poor adhesion of the film and had a greater thickness. Therefore, preference was given to films obtained from solution with low concentration of tin atoms (0.14 mol/L). Thin layers were obtained. By subsequent deposition of additional layers the multilayered films were obtained with good adhesion to glass substrate, acceptable optical properties and resistance of about 200 ohms.

Characteristics of tin oxide films deposited by magnetron sputtering (pressure Ar-O₂ mixture in the chamber –1 Pa) and sol-gel technique were compared. It was found that the relative resistance of films prepared by sol-gel technique, much faster decrease with increasing

temperature (Fig. 9), and the increase of their resistance associated with a decrease in carrier mobility due to scattering by impurities occurs at higher temperatures (> 270°C).

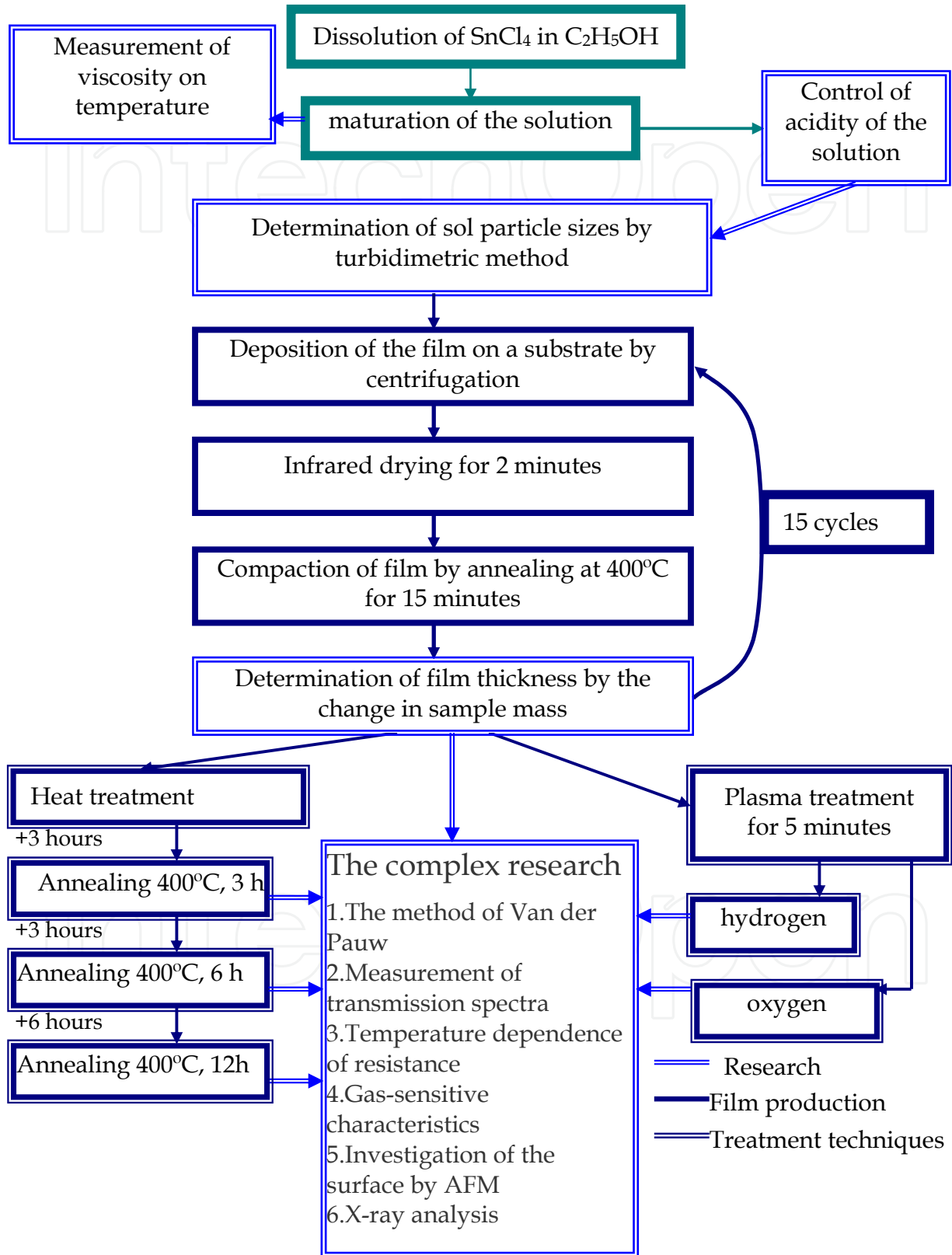


Fig. 8. Scheme of the synthesis and study of nanostructured SnO₂ films (sol-gel technology)

The absolute values of the resistance of films, prepared by magnetron sputtering, changed in the temperature range 20-230°C from 69 to 11 kohm, while for the sol-gel films from 192 to 2.3 kohm. Low resistance of films obtained by magnetron sputtering at room temperature may be due to the presence of particles of tin, whose resistance increases with increasing temperature. On the other hand, the alleged occurrence of dielectric inclusions of tin monoxide may be the cause of the increased resistance of these films at 230°C in comparison with the sol-gel films.

Fig. 10 shows the optical transmission spectra of films obtained in two ways. Transparency of films was about 90%. At long wavelengths there is a reduction of the transmission coefficient for the film SnO_x obtained by magnetron sputtering. The absence of a similar reduction for the films prepared by sol-gel technique indicates a lack of tin particles in films and, consequently, a better stoichiometry of the films of tin dioxide.

Table 2 shows the optical parameters determined from the transmission spectra by ways described in papers (Mishra et al., 2002; Ryzhikov et al., 2002). Films prepared by the sol-gel technique have high porosity, which is considered a positive factor contributing to increase of their gas sensitivity.

The method of film deposition	n, refractive index	D, film thickness, nm	E _g , band gap, eV	ρ, density, g/cm ³	k, absorption coefficient, 1/cm	V, porosity, %
Magnetron sputtering	1.81	282	4.05	5.76	1.67×10 ³	17
The sol-gel technique	1.73	318	4.10	5.35	2.49×10 ³	23

Table 2. Optical parameters of SnO_x film

SnO_x film prepared by magnetron sputtering (pressure of Ar-O₂ mixture in the chamber 1 Pa), after the deposition had an amorphous structure. Annealing in the temperature range 400–550°C led to the formation of polycrystalline phases of SnO₂, SnO, Sn₂O₃ (Fig. 11a). The results help to explain the slow decrease in the resistance of these films with increasing annealing temperature (Fig. 9) by the dielectric properties of the SnO crystallites. The SnO_x film obtained by sol-gel technology had a polycrystalline structure after deposition and short-term annealing at 400°C for 15 minutes, included in the process of drying the film. X-ray diffraction patterns and intensity curves of these films indicate the presence of only polycrystalline SnO₂ phase (Fig. 11b). The crystallites sizes were of the order of 3–5 nm (Table 3), that is more optimal to obtain the gas-sensitive films.

The method of film deposition	SnO ₂ plane	Crystallite sizes, nm
Magnetron sputtering	SnO ₂ (101)	11.4
	Sn ₂ O ₃ (021)	8.5
	SnO (101)	10.0
The sol-gel technique	SnO ₂ (110)	5.2
	SnO ₂ (101)	5.1
	SnO ₂ (211)	3.0

Table 3. Average crystallite sizes of SnO₂ films

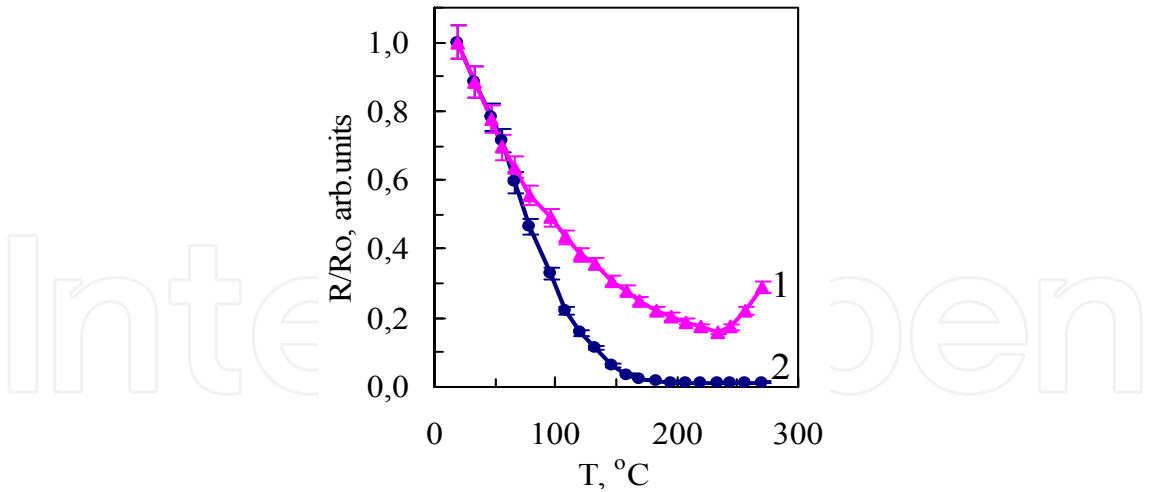


Fig. 9. Temperature dependences of resistivity of the SnO_x films: 1 – film deposited by magnetron sputtering, 2 – by sol-gel method.

Research of gas sensitivity of the deposited films was conducted in two stages. In the first stage, the temperature dependences of film resistance in both pure air, $R_0(T)$, and at a given concentration of the test gas, $R_g(T)$, were measured. It was determined the temperature at which a maximum sensitivity of film to test gas observed. In the second stage, the effects of different concentrations of the gas at this temperature are measured.

Fig. 12 shows curves of temperature dependences of the sensitivity for films synthesized by both sol-gel method and magnetron sputtering, at an ethanol concentration of 1 mg/L. Maximum sensitivity of the sol-gel films to the ethanol vapors is shifted to lower temperatures (230°C), relative to films prepared by magnetron sputtering (270°C). This may be due to smaller crystallites, higher porosity and homogeneity of the phase composition of the sol-gel SnO₂ films.

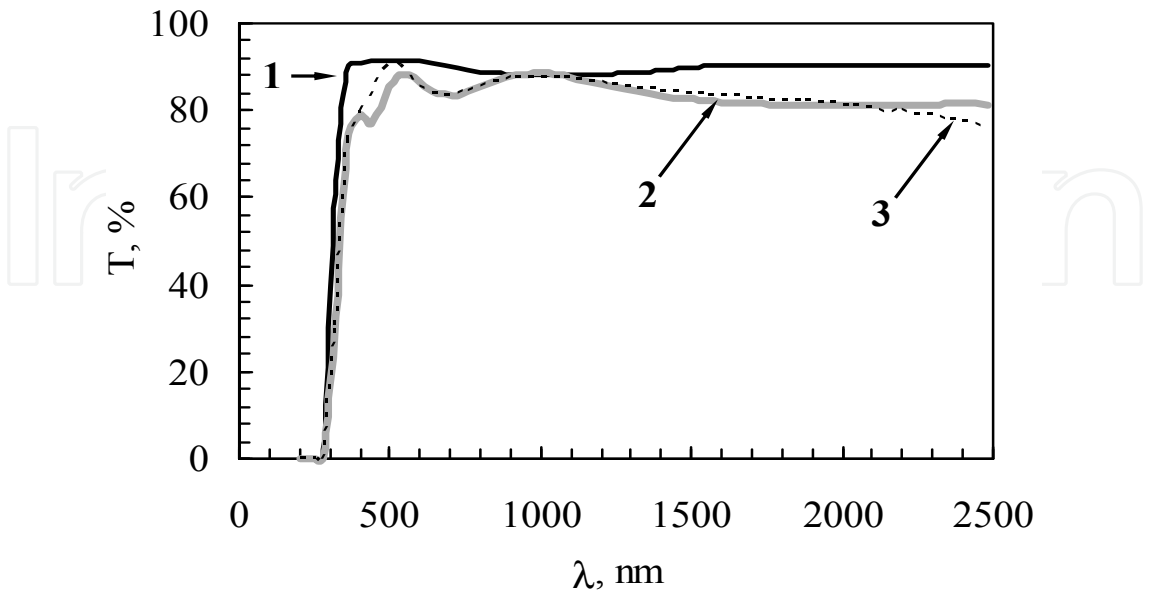


Fig. 10. Optical transmission spectra of SnO_x films: 1 – glass, 2 – film, deposited by the sol-gel technique, 3 – film deposited by magnetron sputtering.

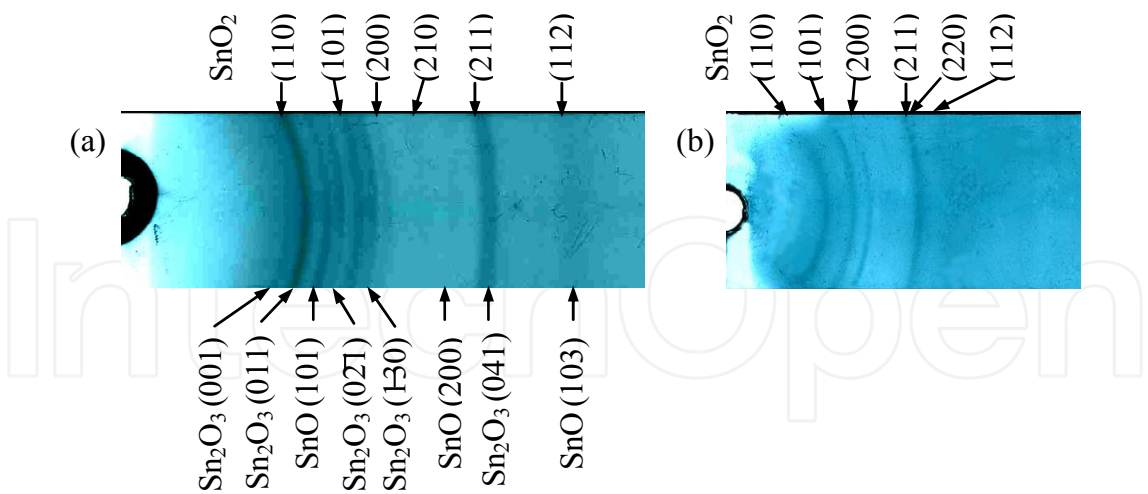


Fig. 11. X-ray diffraction patterns for thin SnO_x films on glass substrates: a) films obtained by magnetron sputtering, and b) by the sol-gel technique.

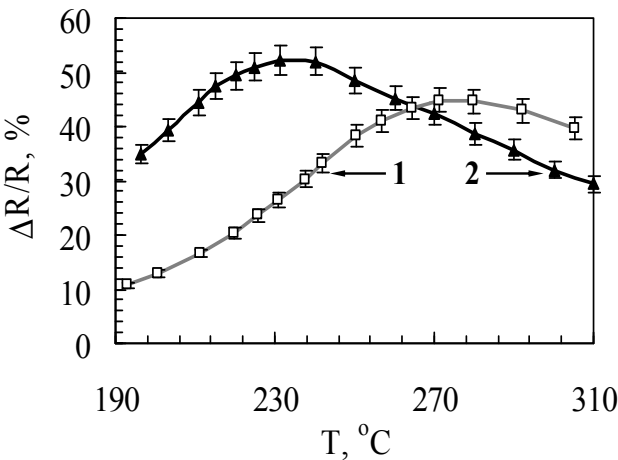


Fig. 12. Temperature dependence of the sensitivity of tin dioxide films to ethanol (concentration 1 mg/L): 1 – film deposited by magnetron sputtering, 2 – by sol-gel technique.

The listed above factors also affect the dynamic performance. To measure the response time of gas-sensitive film, in the volume of the reactor a certain number of identified gas for the time of the order of tenths of a second was introduced. Fig. 13 shows the response time for the presence of ethanol vapor with a concentration of 1 mg/L (500 ppm), for which the film resistance dropped by 90%. For the films obtained by sol-gel method and magnetron sputtering, the response time was ~ 3 and 16 s, recovery time of resistance to the initial value was 70 and 90 s, respectively.

Fig. 14 shows the dependence of sensitivity of the SnO₂ films synthesized by both sol-gel technique and magnetron sputtering, on the concentration of ethanol vapor at a temperature corresponding to the maximum of sensitivity. There is a sensitivity to trace amounts of ethanol vapor of films synthesized by sol-gel technique. In addition, the films have a linear sensitivity to small concentrations of ethanol.

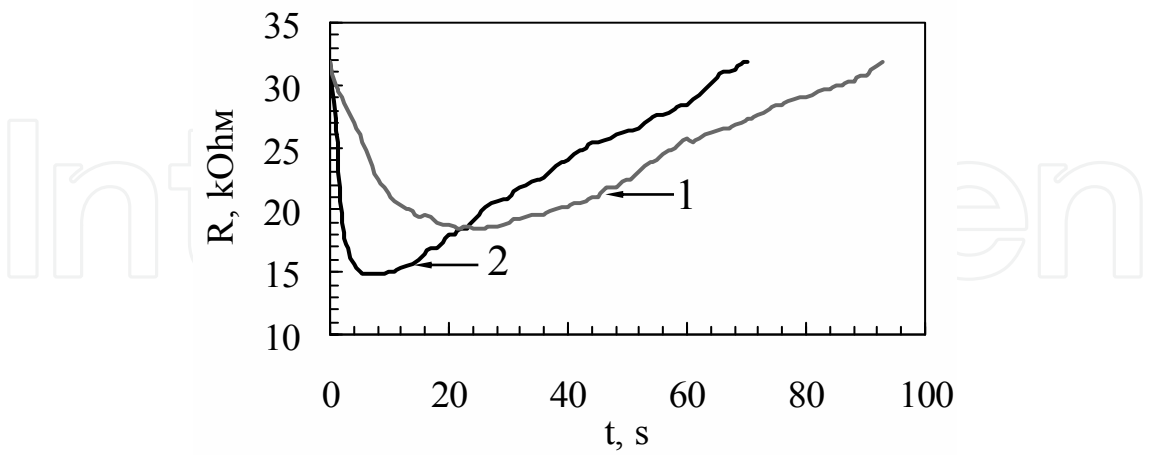


Fig. 13. The dependence of the response time of SnO₂ layer on ethanol vapors (concentration 1 mg/L): 1 – film deposited by magnetron sputtering, 2 – by sol-gel technique.

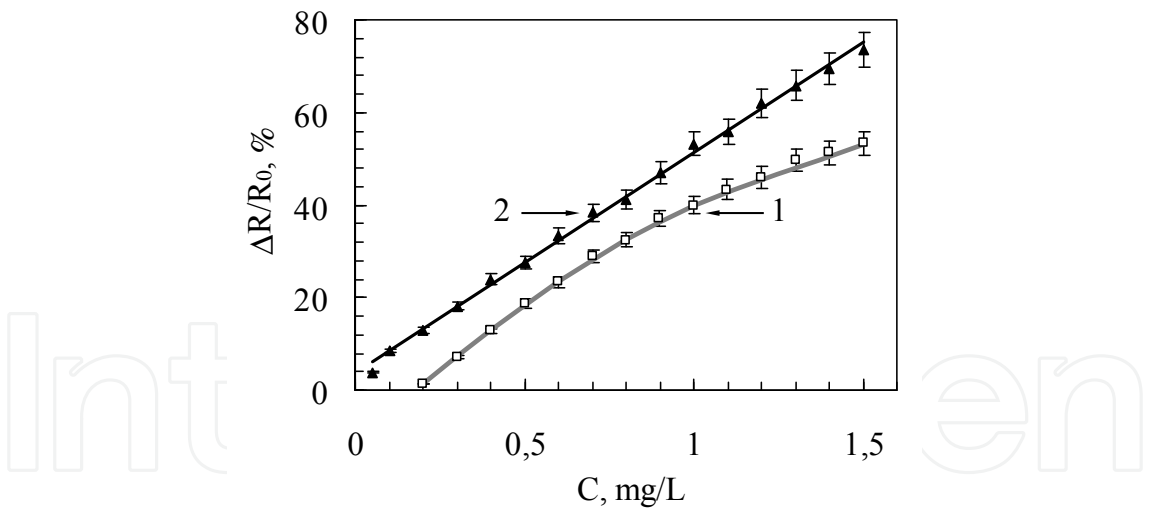


Fig. 14. The dependence of sensitivity of SnO₂ films to the concentration of ethanol vapors: 1 – film deposited by magnetron sputtering, 2 – by sol-gel technique.

Fig. 15 shows the atomic-force microscope images of the surface microstructure of the glass substrate and SnO_x film deposited by magnetron sputtering and sol-gel technique. The film deposited by magnetron sputtering, consists of large agglomerates, and the film synthesized by sol-gel technique has a fine-grained structure of the surface.

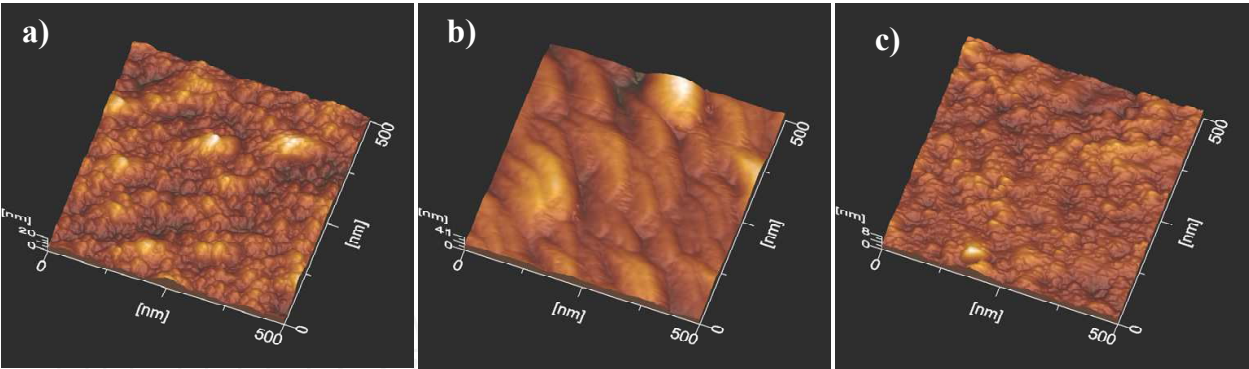


Fig. 15. Surface topography of the SnO_x films on glass substrates: a) glass, b) SnO_x film, deposited by magnetron sputtering, c) by sol-gel technique.

Table 4 presents data on the film surface structure obtained using the processing software to an atomic force microscope, where: R_a is average roughness; R_{zjis} – average roughness of 10 points; S – area of the image; R_q – RMS roughness; R_z – the difference between maximum and minimum height of an image; S_{ratio} – the ratio of the image area S to the area of flat surface S_0 .

Parameters	Microscope slides (glass)	SnO _x films	
		Magnetron sputtering	The sol-gel method
R_a , nm	2.31	3.58	0.66
R_{zjis} , nm	17.7	27.1	5.67
S , nm ²	264632.0	259867.1	251484.2
R_q , nm	2.92	4.69	0.842
R_z , nm	19.0	35.6	7.02
S_{ratio}	1,06	1.04	1.01

Table 4. Parameters of the surface structure of SnO₂ films on glass

3.3 Influences of thermal and plasma treatments on phase composition, microstructure and physical properties of the SnO_x films deposited by sol-gel technique and magnetron sputtering

To modify the properties of SnO₂ films, different ways of their treatment are widely used. Of particular interest is the study on the influence of thermal and plasma treatments on optical and structural properties of the SnO_x films, deposited by the sol-gel techniques.

As is known, the crystallization of SnO₂ films on glass substrate takes place most intense at temperatures of 400–600°C. Heat treatment for 1 hour at temperatures of 550–600°C on energy costs can be equivalent to several hours of treatment at 400°C. However, the changes of the structural and sensory properties of the films may be non-equivalent in these conditions. Analysis of the influence of the duration of isothermal annealing on the properties of the films is of a separate scientific and practical interest.

In recent years, the plasma treatment for modifying the properties of SnO₂ films is used (Karapatnitski et al., 2000). It has been reported about the influence of plasma on the sensitivity of the sensors. An analysis of changes in the optical parameters determined from

transmission spectra in combination with changes of structural characteristics on the basis of X-ray diffraction and atomic force microscopy, may help to better understand the dynamics of the physical and structural properties of thin films of tin dioxide.

This section presents the results of the study of the effect of isothermal annealing (15 min, 3 hours, 6 hours and 12 hours at $T = 400^\circ\text{C}$) and processing by hydrogen and oxygen glow discharge plasma on the microstructure, optical and electrical properties, thickness, porosity and gas sensitivity of SnO_2 films, deposited by the sol-gel technique (the method of centrifugation) on a glass substrate. The results are interpreted by comparing with recent data on the effect of plasma treatment on the properties of films obtained by magnetron sputtering or ion implantation.

3.3.1 Influence of thermal and plasma treatment on phase composition, microstructure and physical properties of the SnO_x films deposited by magnetron sputtering

Fig. 16 shows the dependence of sensitivity on the concentration of ethanol vapor for thin SnO_2 film, obtained by magnetron sputtering, after treatment by oxygen plasma (27.12 MHz, 12.5 W, 6.5 Pa, 100°C , 5 or 20 min). The SnO_2 film acquires a high sensitivity ($> 50\%$) to ethanol vapor with concentrations below 0.2 mg/L after treatment by oxygen plasma for 5 and 20 min. The short-term treatment for 5 min was more effective for increasing the sensitivity of the SnO_2 films ($\sim 70\%$). This significant effect of plasma treatment on the gas-sensitive properties of the SnO_2 films, probably, is caused by changes in the structure of the films during processing.

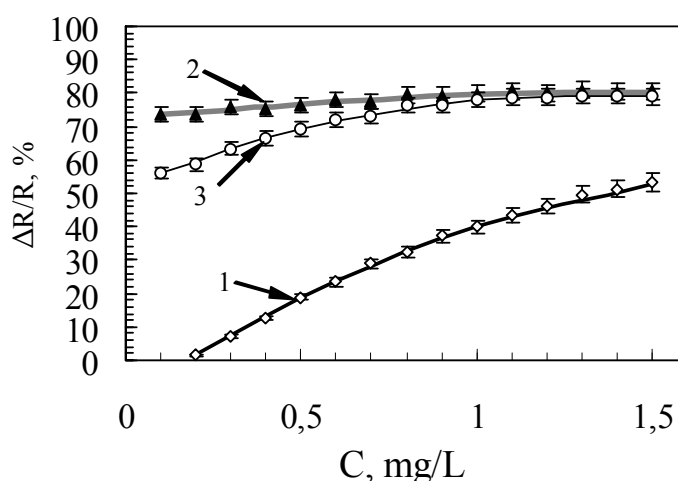


Fig. 16. Dependence of the sensitivity on the concentration of ethanol vapor for SnO_2 film: 1 – after deposition, 2 – after treatment by oxygen plasma for 5 minutes, 3 – for 20 minutes.

As shown in Fig. 17, immediately after the deposition by magnetron sputtering (cathode voltage is 470 V, discharge current – 35 mA, the pressure in a Ar-O_2 mixture in the chamber – 2.7 Pa, oxygen concentration 10%, the rate of deposition of films ~ 0.05 nm/s, substrate temperature 200°C) the films have a nanocrystalline structure and contain SnO_2 crystallites with sizes about 4 nm. In this case there are clear reflections from the systems of planes of SnO_2 with Miller indices (110), (101), (211) and (112). After oxygen plasma treatment for 5

minutes (Fig. 17b) and 20 minutes (Fig. 17c) the intensities of SnO₂ lines are greatly reduced. This may occur due to destruction of crystallites of tin oxide under the influence of oxygen plasma to form a cluster structure of the film. Clustering is not accompanied by appreciable sputtering of the film, since after annealing at 550°C for 1 h the structure of SnO₂ crystallites is restored and the intensity of lines on X-ray Debye patterns almost restored (Fig. 17d). Table 5 shows the optical parameters of the films, calculated by standard methods (Song, 1999). It is seen that the thickness of the film after oxygen plasma treatment decreases slightly.

If the deposition of SnO_x film is carried out in condition of a lack of oxygen at reduced pressure ~ 1 Pa in a Ar-O₂ mixture in the chamber, an increase of the concentration of excess tin in the film results the formation of tin (β-Sn) crystallites with an average size of ~ 30 nm (Fig. 18a) during treatment by hydrogen plasma. So, that demonstrates a segregating effect by hydrogen plasma on the film structure. After annealing of these films in air at 550°C for 1 h, both as-treated and not treated by H-plasma, the appearance of X-ray lines of SnO₂ (6 lines), Sn₂O₃ (5) and SnO (1) phases (Fig. 18b), is observed. Crystallite sizes are in the range of 8-18 nm. Processing of annealed samples by hydrogen plasma led to a blurring of line sections in the angle range of 15° < θ < 20° (in the region between arrows 1 in Figs. 18c and 19), corresponding to reflection from the plane systems of SnO(101), SnO₂ (101) and (200), Sn₂O₃ (021) and (030) . Since the X-ray lines on the Debye photograph are a consequence of a number of specular reflections from the set of crystallites which are in reflecting position in accordance with the equation of Bragg $2d \cdot \sin \theta = \lambda$, the blurring of line sections can occur when selective destruction (amorphization and clusterization) only those crystallites which are oriented to reflect in the area of blurring (between arrows 1). This assumes such orientation of SnO_x film towards the movement of the plasma particles, that the symmetry and arrangement of atoms in the systems of planes of the crystallites SnO(101), SnO₂(101) and (200), Sn₂O₃ (021) and (030) (plane A in Fig. 19) are disordered. The estimation of the angles α between the projection onto a plane perpendicular to the incident X-ray beam, of normals to the sample surface and to the planes A of crystallites which were in the reflecting position before clustering by hydrogen plasma treatment. Angle α for the plane systems SnO(101), SnO₂(101) and (200), Sn₂O₃ (021) and (030) lies in the range of 15–45°, and the angle θ in the range of 15–20°.

Sample	n, refractive index	D, film thickness, nm	E _g , band gap, eV	k, absorption coefficient, 1/cm	V, porosity, %	ρ, density, g/cm ³
Magnetron sputtering	1.830	280	4.05	1.65·10 ³	15.5	5.89
O-plasma	1.750	276	4.05	1.68·10 ³	21.0	5.45
H- plasma	1.805	294	4.05	2.25·10 ³	17.0	5.75

Table 5. The parameters of SnO_x films deposited by magnetron sputtering at a pressure of Ar-O₂ mixture inside the camera – 2.7 Pa, after deposition and treatment by a glow discharge plasma

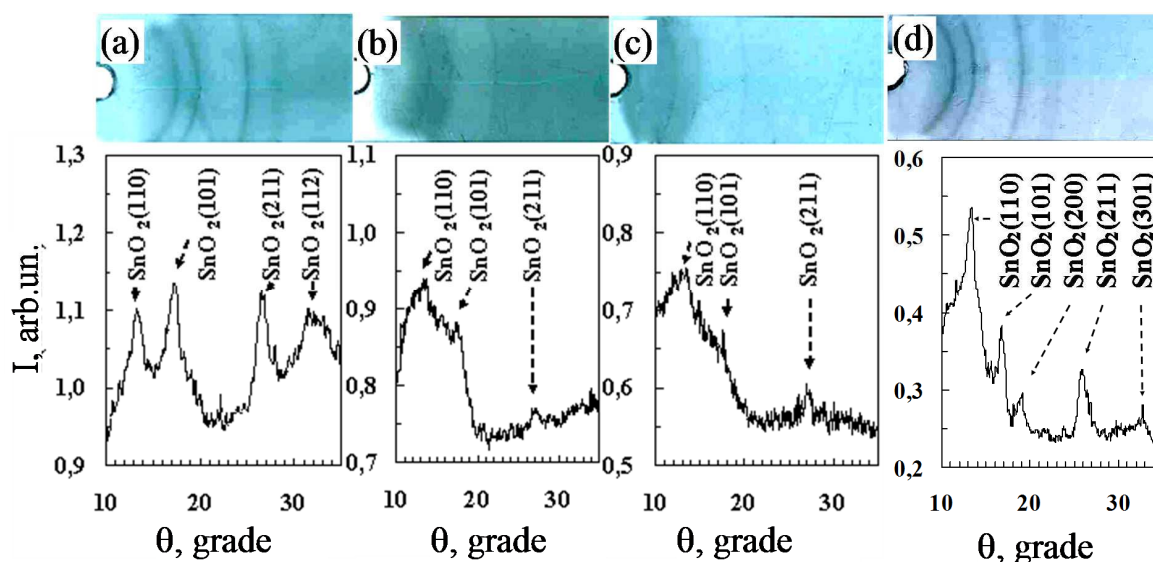


Fig. 17. X-ray diffraction patterns and intensity curves for the thin SnO_2 film after deposition by magnetron sputtering (pressure 2.7 Pa in Ar- O_2 mixture) on a glass substrate (a), after treatment by a glow discharge oxygen plasma for 5 min (b), 20 min (c) and annealing at 550°C for 1 h (d).

In other directions, areas of X-ray lines not subjected to blur (in the region between the arrows 2 in Figs. 18c and 19), the crystallites were solid and even increased their size, demonstrating segregate effects of hydrogen plasma. The order of arrangement of atoms in the systems of planes of $\text{SnO}(101)$, $\text{SnO}_2(101)$ and (200) , Sn_2O_3 in these crystallites (plane B in Fig. 19) is intact. Angle α for these planes lies in the range of $15-(-45)^\circ$, and the angle θ in the same range of $15-20^\circ$. Therefore, the possibility of obtaining by treatment in glow discharge hydrogen plasma of crystal-amorphous nanostructures in which high-quality nanocrystals of tin oxide alternate with nanosized clusters of tin oxides, is shown.

Repeated annealing for 1 h at 550°C (Fig. 20, curve 7) causes the restoration of the integrity of the X-ray lines of $\text{SnO}(101)$, $\text{SnO}_2(101)$ and (200) , $\text{Sn}_2\text{O}_3(021)$ and (130) (Fig. 18d).

It follows from the optical transmission spectra (Fig. 20, curve 2), low pressure of Ar- O_2 mixture in the chamber (~ 1 Pa), which leads to an increase in the concentration of excess tin in the film, leads to a significant deterioration of its transparency. The presence of significant amounts of tin clusters after deposition is probably the reason for the lack of transparency of the films at low wavelengths (< 500 nm) and low transparency in the region above 500 nm, as β -Sn crystallites yet not observed on X-ray patterns. The formation of tin (β -Sn) crystallites with an average size of ~ 30 nm (Fig. 18a) after treatment by hydrogen plasma leads to a further reduction in the transparency of the film (Fig. 20, curve 3) over the entire considered range of wavelengths (500–1100 nm). The decomposition and oxidation of tin crystallites at the subsequent annealing in air at 550°C for 1 h (Fig. 18b) leads to significant increase of film transparency (Fig. 20, curve 4) both in range of > 500 nm, and at small length waves $\sim 350-500$ nm ($T(\lambda)$ from 0 to $\sim 80\%$), for which the film was not transparent. This may be caused not only by oxidation of the β -Sn crystallites, but also tin clusters. At the same time the transparency of these films is higher than the transparency of untreated by H-plasma films after annealing under the same conditions (Fig. 20, curve 5). This may be due

to more intense oxidation processes in the plasma-treated films in the annealing process due to their higher porosity (11.8 instead of 7.7 according to Table 6). As seen from Fig. 20 (curve 6), the processing by H-plasma of the annealed polycrystalline films, leads to a marked deterioration in transmittance in the wavelength range 300–1100 nm. This may be due to disordering of the structure and the formation of crystal-amorphous structure containing opaque inclusions of SnO, in accordance with (1):

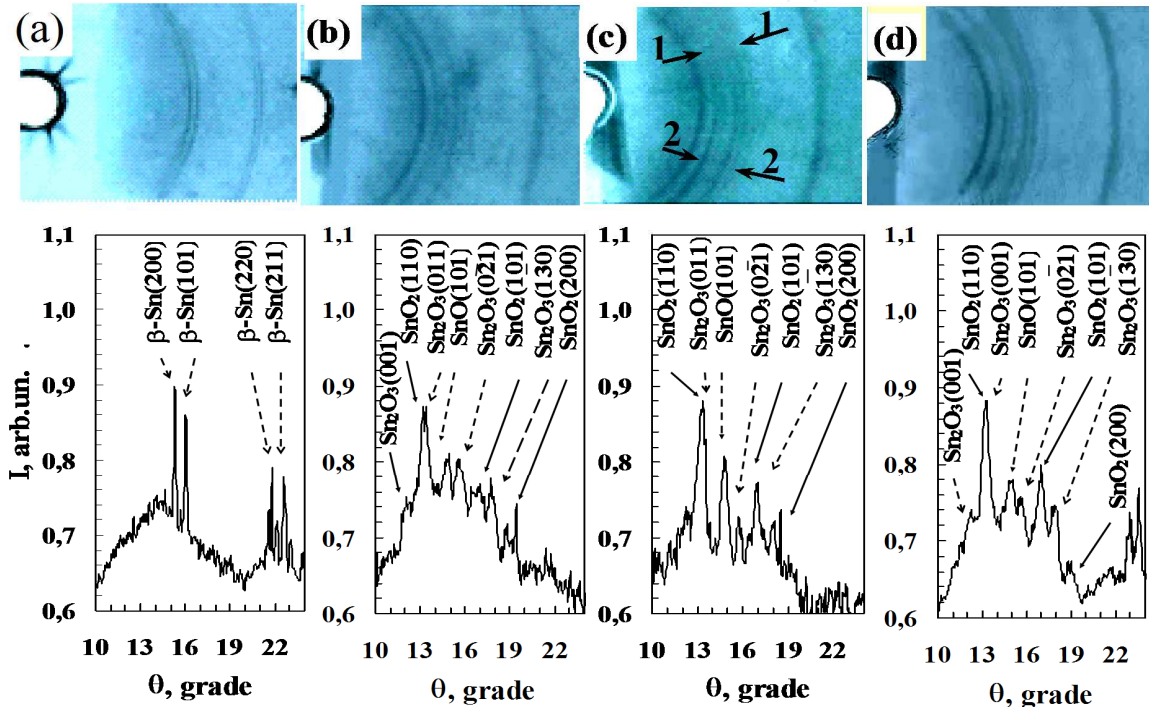
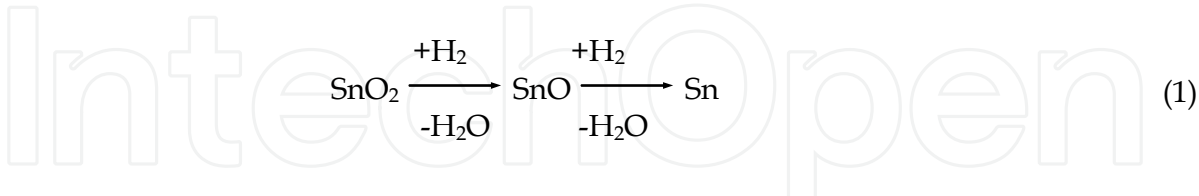


Fig. 18. X-ray diffraction patterns and intensity curves for the SnO_x films after deposition by magnetron sputtering (pressure of 1 Pa in Ar-O₂ mixture) and H-plasma treatment (a), deposition and annealing at 550°C for 1 h (b), the subsequent processing of H-plasma (c) and re-annealing at 550°C (d).

Further annealing at 550°C (1 h) permits to maximize the transparency of the films produced under low pressure in Ar-O₂ mixture in the chamber (~ 1 Pa). This is due to the restoration of the structure of microregions, disordered during plasma treatment. It is assumed that the transformation of these areas during the oxidation into SnO₂ crystallites with a higher density than Sn₃O₄, increases the porosity of the films (Table 6), which is important for the gas sensitivity of films.

The obtained data allows us to interpret the transmission spectra of SnO_x films, obtained by magnetron sputtering under higher pressure in Ar-O₂ mixture in the chamber ~ 2.7 Pa (Fig. 21). X-ray data show the presence of polycrystalline SnO₂ phase immediately after the deposition and the absence of β-Sn crystallites (Fig. 17a). As is seen in the figure 21 (curves 3 and 4), a significant drop in *T*(λ) in range of 1200–2500 nm after processing of the SnO_x films

for 5 min by O-plasma or H-plasma is observed. The decrease of the transmission of these films, consisting mainly of SnO_2 crystallites (Fig. 17a), can occur as a result of increase of the concentration of free charge carriers due to segregation of excess atoms of tin and the formation of tin clusters with sizes of tenths of a nanometer. It should be noted that the phenomenon of reducing of the transparency due to the presence of nanoparticles in the films is less pronounced in the case of oxygen plasma treatment, because the process of segregation of tin nanoparticles is accompanied by a process of oxidation of some part of them up to SnO_2 .

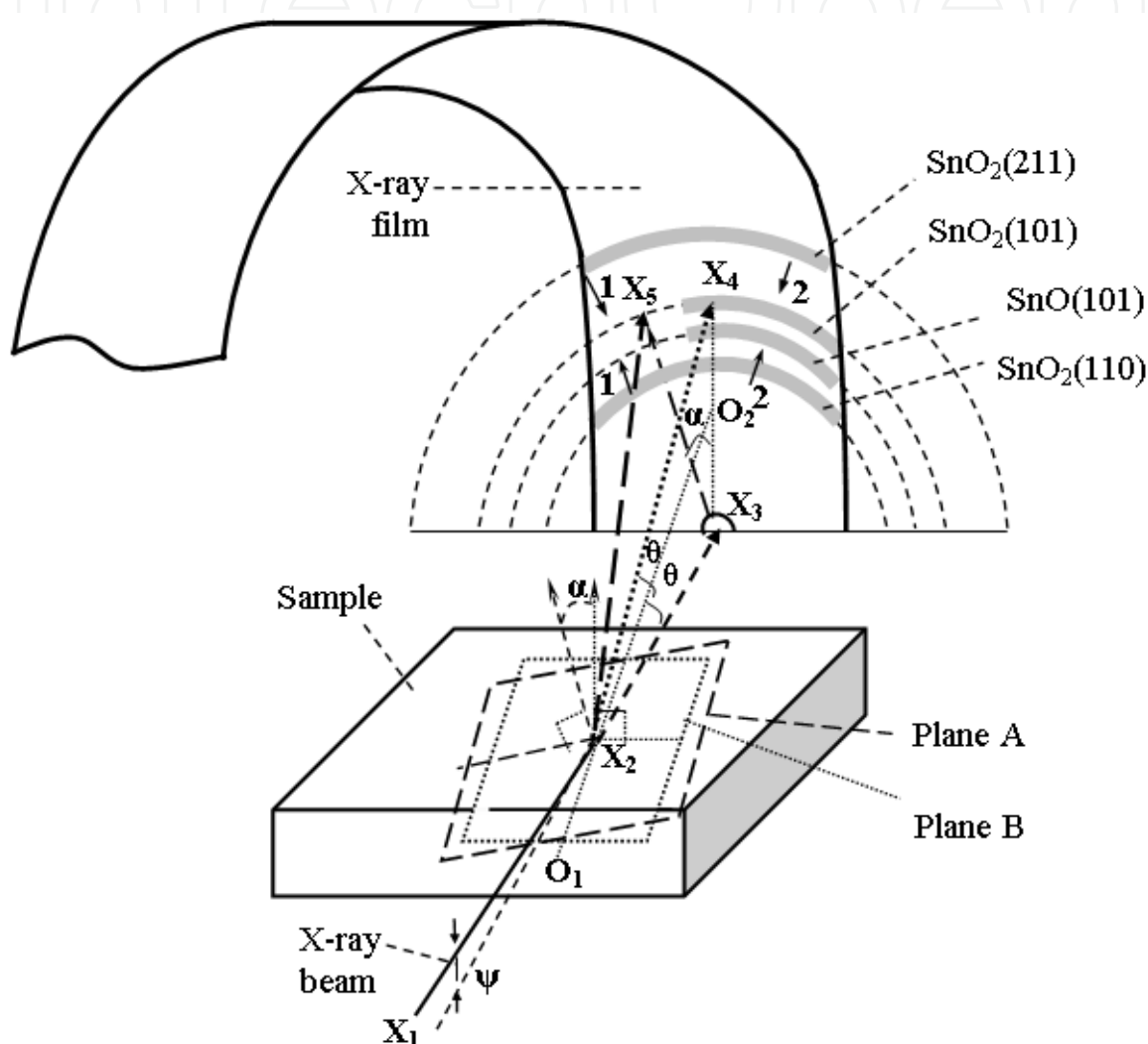


Fig. 19. Illustration of the blurring of X-ray line sections (using $\text{SnO}_2(101)$ and $\text{SnO}(101)$ as an example) in the angle ranges $15^\circ < \theta < 20^\circ$ and $15^\circ < \alpha < 45^\circ$ (in the region between arrows 1) after treatment of the annealed samples by H-plasma. The X-ray beam paths as follows: X_1X_2 is the X-ray beam incident at an angle of $\psi = 5^\circ$ to the sample surface, X_2X_3 is the direction of the transmitted beam, X_2X_4 is the X-ray beam reflected from the $\text{SnO}_2(101)$ plane system of crystallite B (Plane B), X_2X_5 is the beam reflected from the plane system $\text{SnO}_2(101)$ of crystallite A before its destruction by plasma treatment (Plane A). O_1O_2 is the straight line lying in the A plane and making an angle θ with X_2X_3 and X_2X_4 . α is the angle between the projections onto the plane (perpendicular to the incident X-ray beam) of the normals to the sample surface and to the A plane.

Thus established that the short-term treatment (5 min) by O- or H-plasma on the deposited at a pressure of 2.7 Pa SnO₂ film results in the formation of Sn clusters, which reduces the transparency of the film from 80% to 50% and 40%, respectively, in the near infrared region (1200-2500 nm).

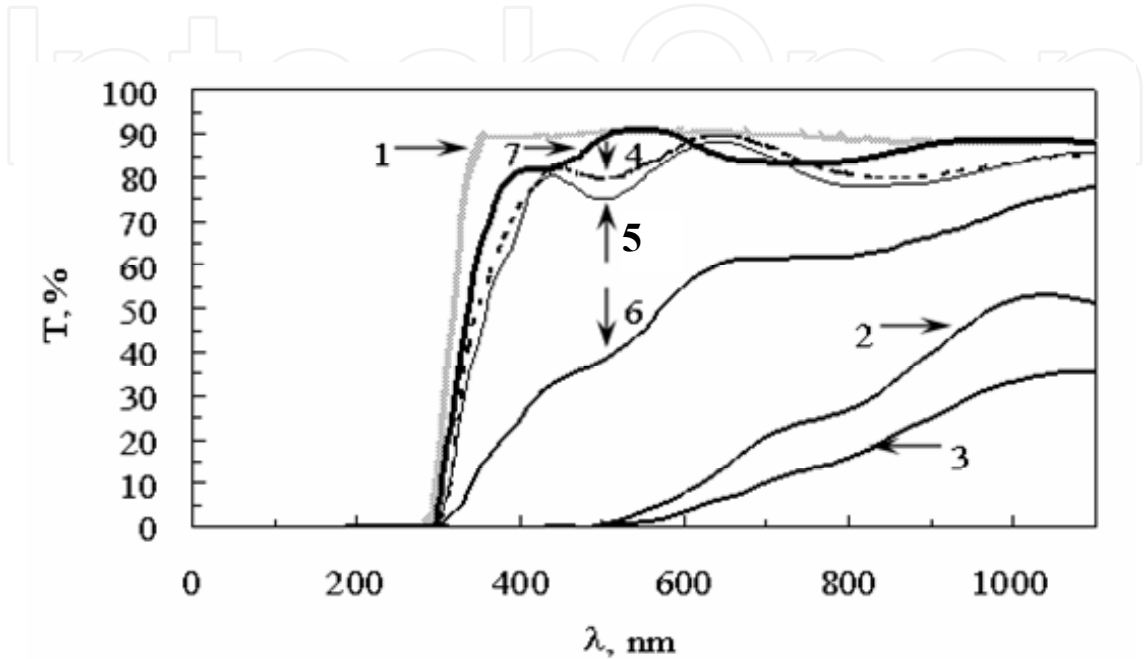


Fig. 20. Optical transmission spectra of glass substrate and thin SnO_x films, deposited by magnetron sputtering (pressure 1 Pa of Ar-O₂ mixture) and treated by H-plasma and annealing: 1 is a spectrum of substrate (glass), 2 – after deposition of SnO_x film on glass, 3 – deposition + H-plasma; 4 – deposition + H-plasma + annealing at 550°C (1 h); 5 – deposition + annealing at 550°C; 6 – deposition + annealing at 550°C + H-plasma; 7 – deposition + annealing at 550°C + H-plasma + annealing at 550°C.

Sequence of operations	n, refractive index	D, film thickness, nm	E _g , band gap, eV	ρ, density, g/cm ³	V, porosity, %
Annealing	1.94	330	4.00	6.42	7.70
Plasma - annealing	1.88	341	4.01	6.13	11.8
Annealing - plasma - annealing	1.82	296	4.05	5.82	16.2

Table 6. Optical parameters of SnO_x film deposited by magnetron sputtering at a pressure of Ar-O₂ mixture in the chamber – 1 Pa

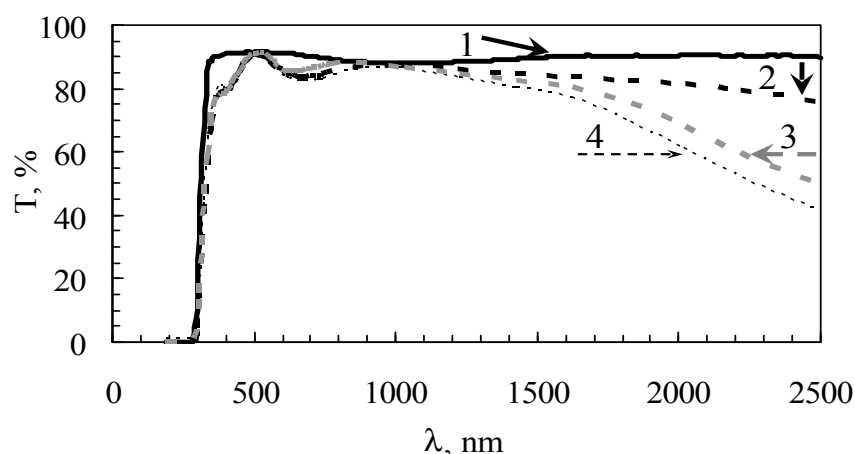


Fig. 21. Optical transmission spectra: the glass substrate (1); thin SnO_x films on a glass substrate after deposition by magnetron sputtering (2) and treatment by oxygen (3) and hydrogen (4) plasma.

3.3.2 Influence of isothermal annealing and plasma treatment on phase composition, microstructure and physical properties of the SnO_x films deposited by sol-gel technique

Colloidal solution for preparation of tin dioxide films was deposited on glass substrate. Rotational speed of the centrifuge was 3800 rpm. Centrifugation time was 3–5 s. The substrates with the deposited films were dried by an infrared emitter at 80°C for 3–5 min. Low temperature annealing was maintained to prevent the occurrence of cracks on the SnO_2 films. Then the sample is placed in a muffle furnace and dried at 400°C for 15 min. The number of deposited layers of SnO_2 was 15. The thickness of the deposited film was estimated from the weight of the film and was about 300 nm.

As shown earlier (Fig. 11b), X-ray diffraction study of SnO_2 films after drying at 400°C for 15 minutes showed that the films have a polycrystalline structure. The structure of SnO_2 crystallites is sufficiently advanced, it contributed to recording X-ray reflections from 6 plane systems with Miller indices SnO_2 (110), (101), (200), (211), (220), (112). The increase of the duration of isothermal annealing leads to an increase in the average size of SnO_2 crystallites in the films: 15 minutes – 6 nm, 3 and 6 hours – little more than 6 nm, 12 hours – more than 10 nm.

Fig. 22 shows the spectra of optical transmission of tin dioxide films after annealing at 400°C for 15 min, 3, 6 and 12 hours. Fig. 23 shows the spectra of optical transmission after treatment by oxygen and hydrogen plasma.

The prepared films have high transparency ($\sim 90\%$). With increasing of annealing time the transparency at short wavelengths is increased, which indicates the improvement of the stoichiometry of tin dioxide films and the removal of residual solvent (Fig. 22). As shown in Table 7, the increase of isothermal annealing time to 6 and 12 h leads to compaction of the film, reducing its thickness, porosity and absorption coefficient.

The treatment by glow discharge hydrogen plasma resulted in a decrease in the transparency on 3–15% in the short-wave range (Fig. 23, curve 4), while the oxygen plasma

treatment resulted in a slight decrease of 1–5% (Fig. 23, curve 3). Noticeable decrease in the transparency of the thin film after hydrogen plasma treatment can be attributed to the formation of opaque compounds such as SnO or Sn, formed by reducing properties of hydrogen in accordance with the reaction (1).

However, X-ray diffraction data do not confirm the presence of crystallites of SnO and Sn in the films treated by hydrogen plasma (Table 7). Nevertheless, the presence of SnO inclusions in the amorphous state or in the form of clusters is possible that leads to an increase in the absorption coefficient from $2.5 \cdot 10^3$ up to $5.91 \cdot 10^3 \text{ cm}^{-1}$ (Table 7). The presence of metal clusters of tin in appreciable amounts is unlikely, since there is no reduction of the transmission coefficient $T(\lambda)$ in the range 1200–2500 nm, associated with an increase in the concentration of free charge carriers.

The treatment by oxygen plasma does not result the formation of SnO, and the slight change in the transparency of the film is caused by the damaging effects of plasma on the structural perfection and crystallite size. Reducing the size of the SnO₂ crystallites is caused by the destructive influence of the massive oxygen ions on the structure of the crystallites (Table 7). The increased density of the film in proportion to the reduction of its thickness is presumably caused by the filling of intergranular voids by SnO₂ clusters. The increase of the SnO₂ crystallites sizes during processing by hydrogen plasma is caused by the segregating effect of light hydrogen ions of plasma, under the influence of which the alteration, destruction, and merging of the crystallites are taken place. Reducing the thickness by 10% while maintaining the density of the film can be occur through the formation and desorption of H₂O molecules and the formation of oxygen vacancies. The formation of SnO molecules on the surface of SnO₂ crystallites is taken place; thereby the stoichiometry and transparency of the film are reduced.

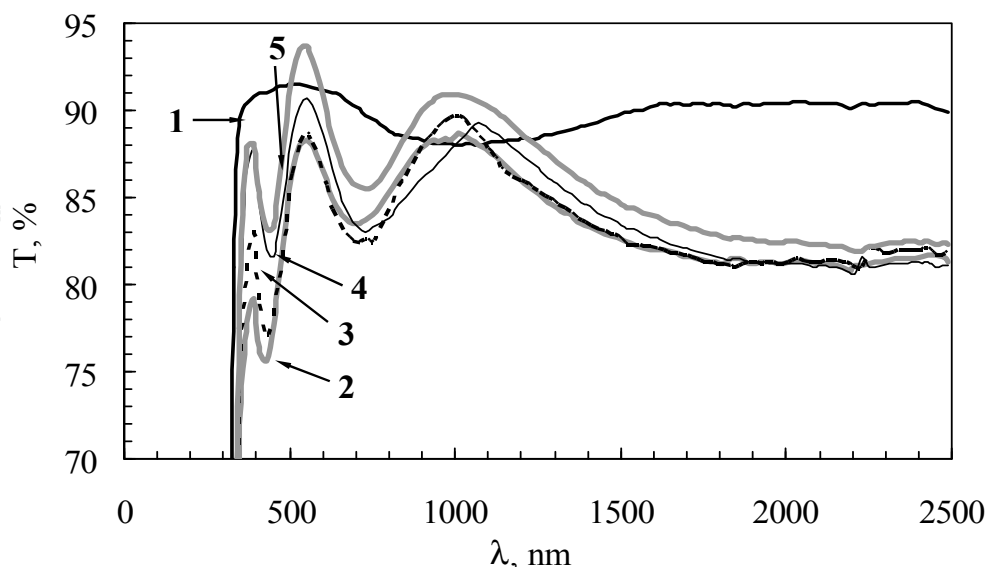


Fig. 22. Optical transmission spectra of SnO₂ films after isothermal annealing at 400°C: 1 – glass substrate, 2 – the film after deposition and annealing for 15 minutes, 3 – 3 hours of annealing; 4 – 6 hours of annealing, 5 – 12 hours of annealing.

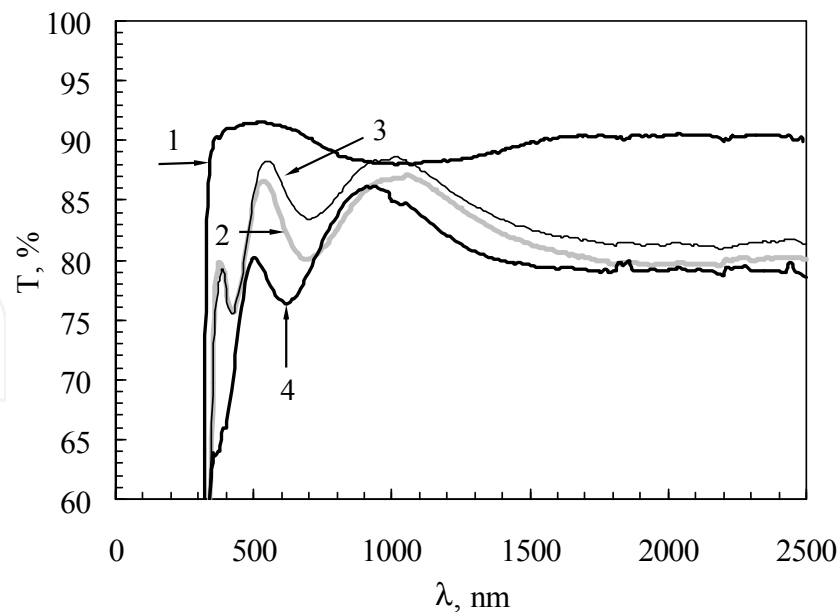


Fig. 23. Optical transmission spectra of SnO₂ films after plasma treatment: 1 – substrate, 2 – after film deposition, 3 – after treatment by oxygen plasma, 4 – after treatment by hydrogen plasma.

Optical and structural parameters		Isothermal annealing				Plasma treatment		
		400°C, 15 min	400°C, 3 h	400°C, 6 h	400°C, 12 h	400°C, 15 min	O-plasma	H-plasma
n, refractive index		1.72	1.76	1.81	1.81	1.74	1.81	1.73
D, film thickness, nm		319	312	304	304	316	297	288
E _g , band gap, eV		4.1	4.1	4.1	4.1	4.1	4.1	4.0
P, density, g/cm ³		5.29	5.53	5.76	5.76	5.40	5.80	5.36
k, absorption coefficient, 1/cm		2.4 · 10 ³	2.3 · 10 ³	1.6 · 10 ³	0.6 · 10 ³	2.5 · 10 ³	3.05 · 10 ³	5.91 · 10 ³
V, porosity, %		23.9	20.5	17.2	17.1	22.3	16.5	22.8
Average size ε of crystallites, nm	SnO ₂ (110)	5	7.5	6	8	5	5.5	6.5
	SnO ₂ (101)	6.5	7	6.5	10	6.5	6	9.5
	SnO ₂ (211)	6	6	6	14.5	6	4.5	10

Table 7. Optical and structural parameters of SnO₂ films

The surface resistance of SnO₂ films after deposition and annealing at 400°C for 15 minutes by four-probe method is measured, and it was 16 ohm · cm (Fig. 24). The surface resistance of the SnO₂ film increases linearly with increasing duration of isothermal annealing (400°C). Resistance measurements were performed at room temperature (22°C). It is seen that each hour of annealing leads to an increase in surface resistance of ~ 24 kohm · cm (Fig. 24). This may be due to a decrease in the number of oxygen vacancies as a result of improving of the crystallite structure and stoichiometry during the long process of annealing in air.

After treatment in oxygen plasma, the film sheet resistance increased from 16 to 133 kohm·cm, apparently due to reducing the number of oxygen vacancies. In contrast, after treatment by hydrogen plasma, it decreased from 16 to 0.7 kohm·cm, presumably due to increase in the number of oxygen vacancies.

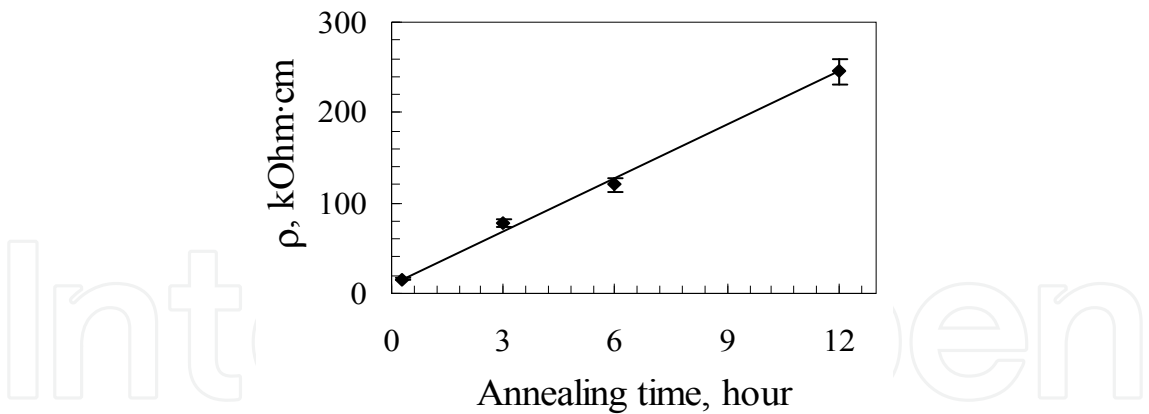


Fig. 24. The dependence of sheet resistance (22°C) of the SnO₂ film on the duration of isothermal annealing at 400°C.

Fig. 25 shows the temperature dependence of the resistance of the films after isothermal annealing, and Fig. 26 - after treatment by hydrogen and oxygen plasmas. The substrate with the film placed on a heated table, located in a cylindrical chamber. The resistance of the deposited films decreases rapidly with increasing temperature (Figs. 25 and 26, curves 1). Increase of the duration of isothermal annealing has little influence on the temperature dependence of resistance (Fig. 25, curves 2–4).

The processing of the film by hydrogen plasma leads to an increase in the number of oxygen vacancies and, correspondingly, a decrease in resistance from 192 kohm to 3.1, resulting in a decrease to 1.6 kohm of resistance with increasing temperature is smooth and the relative resistance decreases slowly (Fig. 26, curve 3). Treatment by oxygen plasma leads to occurrence of excess oxygen in the film and, accordingly, to increase resistance from 192 to 640 kohm, resulting in a decrease to 1.9 kohm of resistance with increasing temperature is faster due to the desorption of excess oxygen (Fig. 26, curve 2).

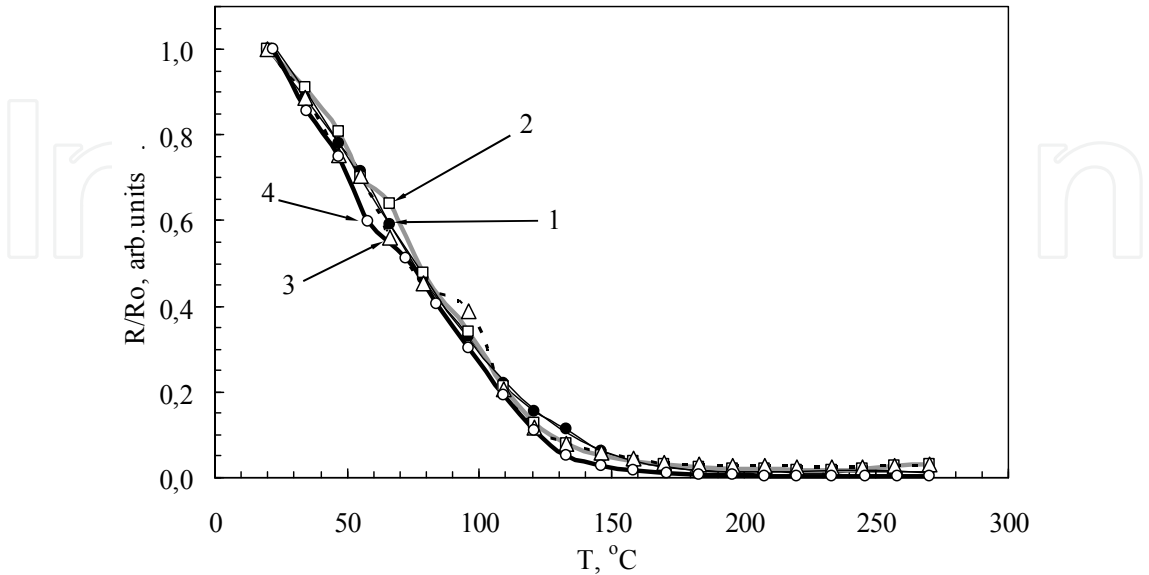


Fig. 25. Temperature dependences of the resistance of the SnO₂ film after annealing at 400°C for 15 minutes (1 - ●), 3 hours (2 - □), 6 hours (3 - Δ) and 12 hours (4 - ○).

Thin films of SnO_2 , subjected to isothermal annealing and plasma treatment, were investigated for sensitivity to ethanol vapor. Gas sensitivity in this case defined as the ratio

$$\gamma = \frac{R_0}{R_g}, \quad (2)$$

where R_0 is resistance of gas-sensitive layer in the clean air, R_g is the resistance of the layer in the mixture of air with detectable gas.

Fig. 27 shows the temperature dependence of the sensitivity for films synthesized by sol-gel technique at concentration of ethanol 1 mg/L after isothermal annealing (a) and treatment by plasma (b). Maximum sensitivity of the sol-gel films to the vapors of ethanol takes place at a temperature of 235°C (Fig. 27, curves 1). There is a significant increase in sensitivity of the films both after annealing and after treatment by plasmas. The maximum sensitivity of the films is observed after annealing at 400°C for 6 hours. A significant decrease in sensitivity after annealing for 12 hours in comparison with annealing for 3 and 6 hours may be due to a significant increase in the crystallite size from ~ 6.5 to ~ 11 nm. As shown by Xu et al. (1991), optimal crystallite size for good gas sensitivity should be ~ 6 nm.

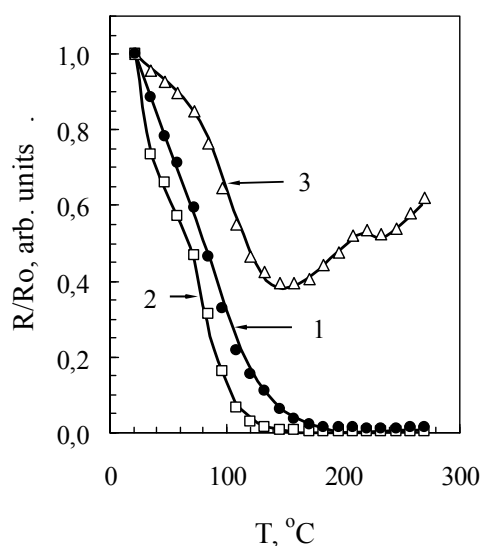


Fig. 26. Temperature dependences of the resistance of the SnO_2 film after deposition (1) and glow discharge oxygen (2) and hydrogen (3) plasma treatment for 5 min.

After processing by plasma, the sensitivity increases without increase of the operating temperature. The observed increase in sensitivity can be caused by an increase in the size of pores and cracks during the bombardment by ions of oxygen or hydrogen. The sensitivity of the films increases linearly (Fig. 28), if the concentration of ethanol vapor increases from 0.05 to 0.8 mg/L and above, after which saturation occurs. The growth of sensitivity is more intense after annealing or plasma treatment. The most intensive growth was observed after annealing for 3–6 hours. A marked sensitivity of the film is evident even when the concentration of ethanol vapor is less than 0.05 mg/L. Response time of sensor to ethanol with concentration of 1 mg/L is decreased from 5 to 2 sec both with the increase of annealing time and when exposed to plasma (Table 8). The recovery time of resistance to the initial value increases from 90 up to 140 s, except the 12-hour annealing (75 s).

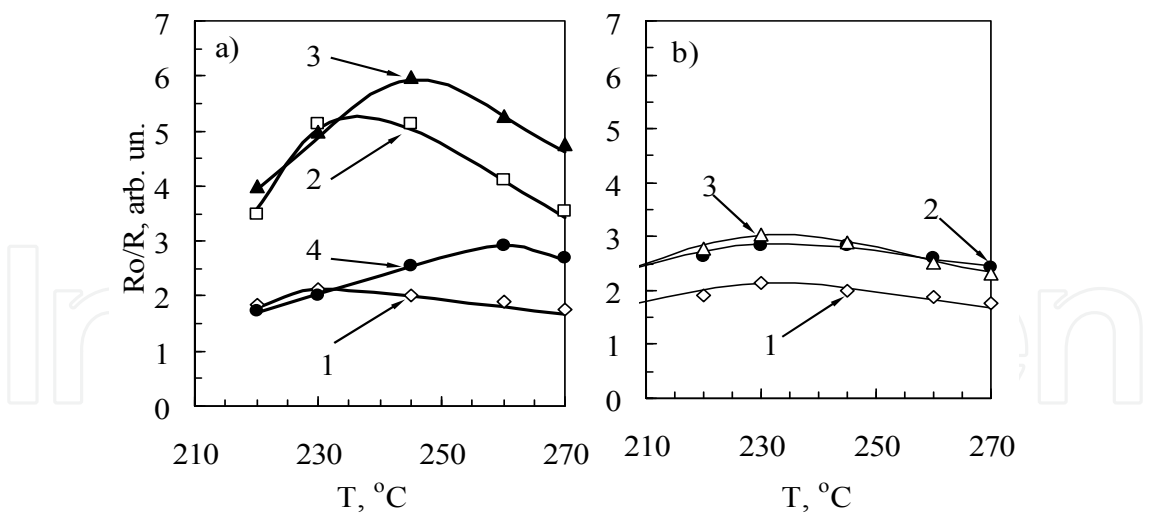


Fig. 27. Temperature dependence of sensitivity to the vapors of ethanol (1 mg/L) of the SnO₂ films: a) after annealing at 400°C for 15 minutes (1), 3 hours (2), 6 hours (3) and 12 hours (4); b) after annealing at 400°C for 15 minutes (1) and treatment by oxygen (2) and hydrogen (3) plasmas for 5 minutes.

The parameters of sensitivity of SnO ₂ films	Isothermal annealing (400°C)				Plasma treatment		
	15 min	3 h	6 h	12 h	400°C, 15 min	O-plasma	H-plasma
Response time, s	5	3	2	2	5	2	3
Recovery time, s	90	140	130	75	90	110	100

Table 8. Response time and recovery time of SnO₂ films

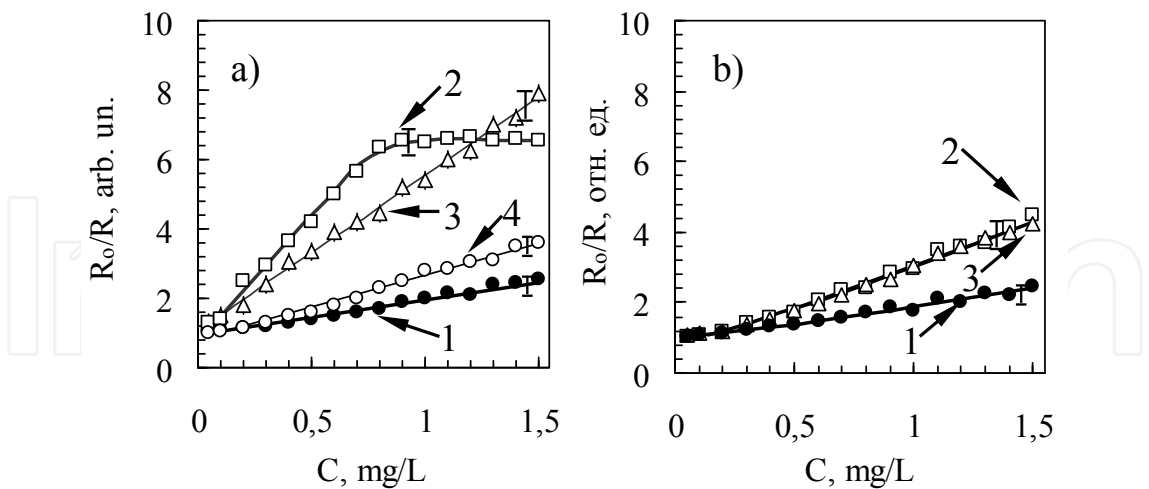


Fig. 28. The dependence of sensitivity on the concentration of ethanol vapor of SnO₂ film: a) after isothermal annealing at 400°C for 15 min (1), 3 h (2), 6 h (3) and 12 hours (4); b) after annealing at 400°C for 15 min (1) and treatment by oxygen (2) and hydrogen (3) plasmas for 5 min.

AFM images of the surface of tin dioxide multilayer film of size 500 × 500 nm (Fig. 29), annealed at 400°C for 15 minutes, 3, 6 and 12 hours, suggest a fine-grained structure of the

film surface. It turned out that after annealing at 400°C for 15 minutes about 80% of the areas of film surface lies at elevations of 1.8–3.7 nm, after annealing for 3 hours – in the range 2.4–4.9 nm, for 6 hours – in the range of 2.7–4.9 nm and 12 hours – in the range of 3.2–6.4 nm. After annealing for 3 and 6 hours on the film surface are observed pronounced granules (Fig. 29b, c). After annealing for 12 hours the surface contains a large number of projections.

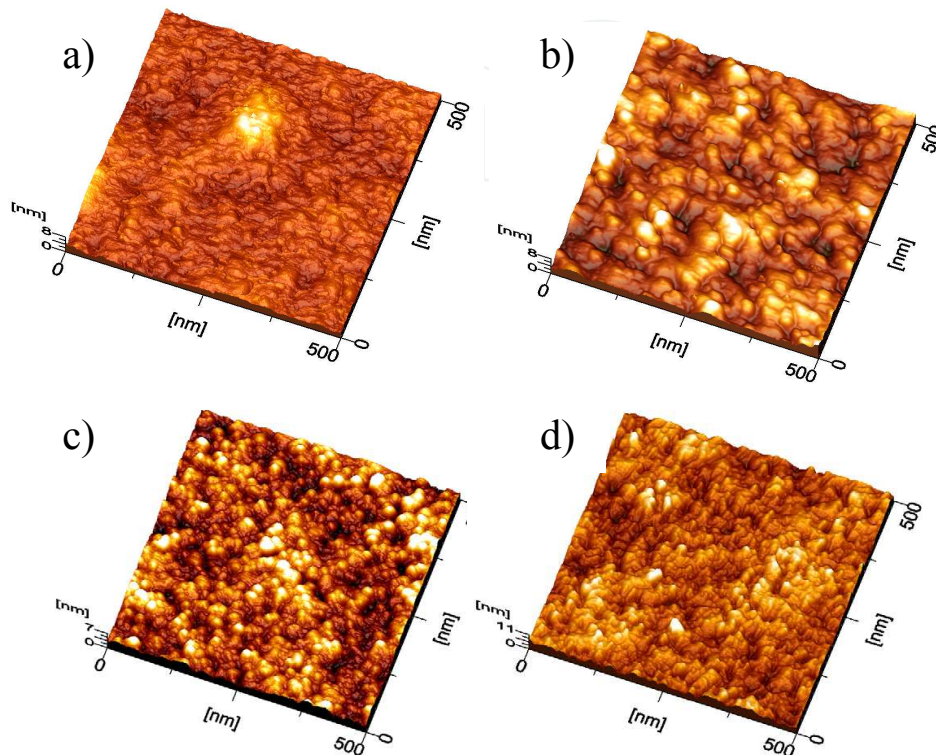


Fig. 29. Surface topography of the films of tin dioxide of 500×500 nm after annealing at 400°C for 15 min (a), 3 h (b), 6 h (c) and 12 h (d).

Treatment by oxygen plasma (Fig. 30b) leads to the disintegration of the granular structure of the film, confirming the assumption about the clustering of structure. Treatment by hydrogen plasma (Fig. 30c) leads to the formation of agglomerates of sizes up to 200 nm. The dimensions of the agglomerates is much greater than the dimensions of the SnO₂ crystallites (~ 9 nm), ie the agglomerates are composed of SnO₂ crystallites.

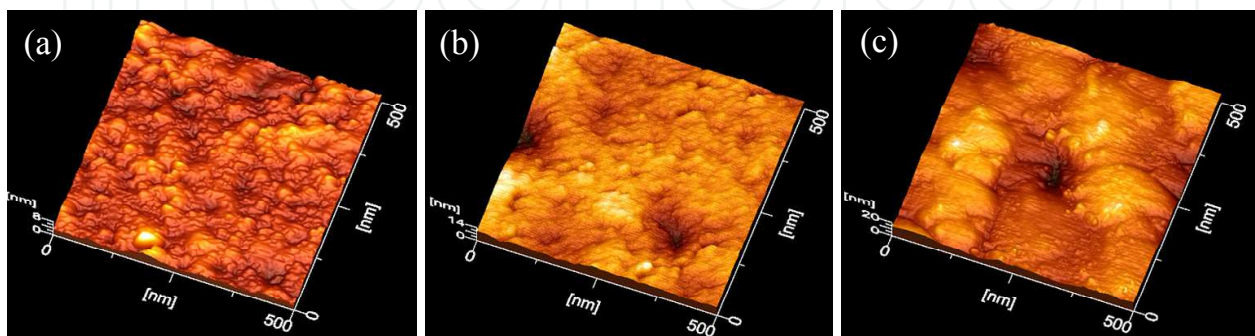


Fig. 30. Surface topography of SnO₂ film after after deposition and annealing (400°C, 15 min) (a) and treatment by O-plasma (b) and H-plasma (c) for 5 min.

Table 9 presents data on the effect of isothermal annealing and treatment by plasma on the roughness of the SnO₂ films, where R_a is average roughness; R_{zjis} - average roughness of 10 points; R_q - RMS roughness; R_z - the difference between the maximum and minimum height of an image. The roughness of the SnO₂ films is increased both after isothermal annealing and after the plasma treatment. This increases the gas sensitivity of film (Figs. 27b and 28b, curves 2 and 3) because the growth of roughness increases the surface area of the film. However, after isothermal annealing roughness varies slightly, but sensitivity is increased more significantly.

Sample	R_a , nm	R_{zjis} , nm	R_z , nm	R_q , nm
Glass substrate	2.31	17.7	19.0	2.92
400°C, 15 min	0.66	5.67	7.02	0.84
400°C, 3 h	0.79	6.32	6.93	0.98
400°C, 6 h	0.74	6.49	7.14	0.93
400°C, 12 h	1.02	9.06	10.0	1.27
400°C, 15 min	0.66	5.67	7.02	0.84
O- plasma	1.15	12.3	13.6	1.58
H- plasma	2.04	16.5	19.7	2.61

Table 9. Analysis of the surface topography of SnO₂ films (500 × 500 nm)

The essential differences in the films deposited by magnetron sputtering and sol-gel technique, include the composition, structure and stoichiometry influencing the properties of the films after deposition as well as after treatment. The comparison of the effect of treatment by hydrogen or oxygen plasma on the individual properties of the SnO₂ films, obtained by these methods, is of particular scientific and practical interest.

Sensitivity to ethanol vapor of films prepared by sol-gel technique, exceeds the sensitivity of the films obtained by magnetron sputtering (Fig. 31, curves 4 and 1). The maximum sensitivity of the sol-gel films at temperature ~ 235°C reaches up to 53%. Treatment by both H-and O-plasma (Fig. 31, curves 5 and 6) increases the sensitivity of the film up to 66% at

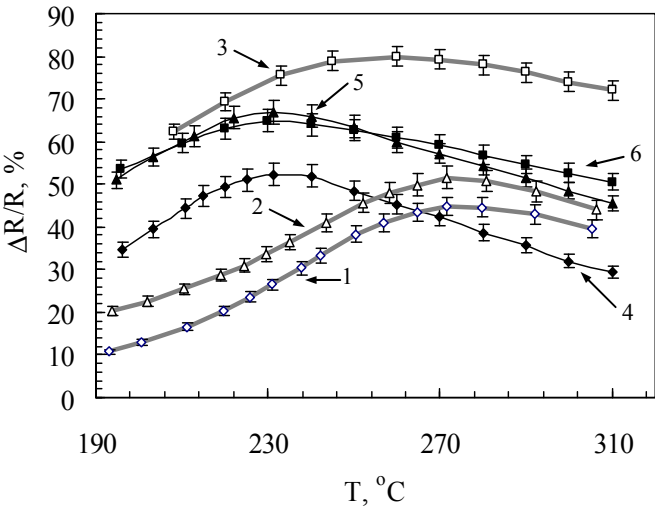


Fig. 31. Temperature dependence of sensitivity to the vapors of ethanol (1 mg/L) of the SnO_x films after deposition by magnetron sputtering (1), H-plasma treatment (2) and O-plasma (3); deposition by sol-gel method (4), H-plasma (5) and O-plasma (6) treatment.

the same operating temperature. For the films synthesized by magnetron sputtering, at an operating temperature of 270°C sensitivity is about 45% (Fig. 31, curve 1). Treatment of H-plasma increases the sensitivity to 52% at the same operating temperature, the same treatment on oxygen plasma increases the sensitivity up to 78% with a decrease in operating temperature to 255°C (Fig. 31, curves 2 and 3).

Thus, the regularities of the influence of treatment by H- or O-plasma on growth of the gas sensitivity of SnO₂ films were established. The plasma treatment of SnO₂ films, obtained by the sol-gel technique, does not alter their phase composition, resulting in gas sensitivity growth does not depend on the type of plasma. Treatment by O-plasma of films prepared by magnetron sputtering, leads to a more significant increase in gas sensitivity than by H-plasma, due to the oxidation of SnO_x film.

4. Conclusion

The problem of modifying the structural properties of the SnO_x films by treatment in glow discharge plasma is studied. Treatments by hydrogen and oxygen plasma permit significantly improve the transparency and gas sensitivity of the SnO_x films. The conditions of film synthesis were revealed, which allow by sol-gel technique (400°C, 6 h) to synthesize the SnO₂ films with high gas sensitivity, the minimum response time (2 seconds) and the optimum crystallite size (6 nm); by magnetron sputtering (10% of O₂ in ArO₂ mixture, 2.7 Pa) to deposit the SnO₂ films with optimum properties (average grain size ~ 4 nm, the transparency ~ 90%, band gap ~ 4.0 eV, the refractive index ~ 1.8) without annealing.

1. A method of formation of the cluster structure of film deposited by a way of spreading, and decrease the average SnO₂ crystallite size up to 1.5 nm by increasing the concentration of tin ions in the film-forming solution from 0.14 to 0.83 mol/L, was developed. This leads to an increase in film sensitivity to the ethanol vapors on 20% (for 1 mg/L), decrease of response time in half (up to 3 seconds) and to appearance of sensitivity to the presence of micro-amounts of ethanol vapor (~ 0.05 mg/L). If the concentration of tin atoms in solution is low (0.14 mol/L), the SnO₂ nanocrystals in film after deposition, drying (100°C, 2.5 nm) and annealing (400°C, 5 nm) were formed.
2. The surfaces of films produced by sol-gel technique (centrifugation method) and magnetron sputtering are fine-grained and in the form of large agglomerates, have an average roughness of 0.6 and 3.6 nm, respectively. The maximum sensitivity of films to the vapors of ethanol is observed at temperatures of 230 and 270°C, the response time is ~ 3 and 16 s, recovery time ~ 70 and ~ 90 s, respectively. The differences may be due to smaller crystallites, higher porosity and the absence of SnO crystallites in the films prepared by sol-gel technique. The treatment by hydrogen plasma of these fine-grained films leads to the formation of large agglomerates. The same treatment by oxygen plasma leads to the disintegration of the granular surface structure and a partial clustering of the film. Isothermal annealing at 400°C for 3–6 h leads to the formation of a pronounced granular surface structure. Treatment by hydrogen plasma of coarse grained (~ 60–120 nm) films, synthesized by magnetron sputtering, leads to a slight decrease in the size of the agglomerates, whereas the treatment by oxygen plasma leads to the destruction of the grains and the film clusterization.

3. The lower resistance at room temperature of films deposited by magnetron sputtering is caused by the presence of tin particles, and a smoother decrease of resistance with increasing temperature is caused by the inclusions of SnO. Films synthesized by the sol-gel technique are composed entirely of SnO₂ phase, have optimal crystallite sizes (3-5 nm) and high values of porosity for higher gas sensitivity. There is no decrease in transmittance at long wavelengths due to absence of tin particles. After treatment by oxygen plasma the excess oxygen atoms increases the film resistance, and its rapid decrease is caused by the desorption of excess oxygen with increasing temperature and absence of SnO inclusions. The treatment by hydrogen plasma results in formation of oxygen vacancies and a decrease of film resistance.
4. It is shown that tin dioxide films synthesized by sol-gel method, after isothermal annealing at 400°C for 15 min, 3, 6 and 12 h have a high transparency (~ 80–90%). The optimum mode of thermal annealing (400°C, 6 h) of SnO₂ films is identified, which permits to achieve the maximum of gas sensitivity and minimum of response time (2 seconds) due to the better structure and optimal sizes (6 nm) of the crystallites.
5. Treatment by glow discharge hydrogen plasma of tin dioxide films synthesized by sol-gel technique resulted in a decrease in the transparency of 3–15% in the visible wavelength range due to the formation of opaque inclusions of SnO. Treatment by oxygen plasma resulted in a slight decrease in the transparency of 1–5% due to the damaging effects of plasma on the structural perfection of the SnO₂ crystallites.
6. For nonstoichiometric SnO_x films ($x < 2$), deposited by magnetron sputtering in condition of a lack of oxygen (pressure Ar/O₂ mixture 1–2 Pa), the formation of polycrystalline β -Sn phase after treatment by H-plasma is shown. Both the segregation of Sn particles at temperatures of 150–200°C and the formation of oxides SnO, Sn₂O₃ and SnO₂ at temperatures of 50–550°C, are taken place. The short-term treatment (5 min) by O- or H-plasma of deposited at a pressure of 2.7 Pa SnO₂ film leads the formation of Sn clusters, which reduces the transparency in the near infrared region (1200–2500 nm) from 80% to 50% and 40%, respectively.
7. The possibility of obtaining of the crystal-amorphous nanostructures in which crystallites of tin oxides alternate with clusters obtained by selective amorphization of SnO, SnO₂ and Sn₂O₃ crystallites during treatment by glow discharge H-plasma, is shown. In this case, the order of the atoms in those (hkl) planes of crystallites is violated, along which there are variations of the plasma particles.
8. The regularities of the influence of treatment by H- or O-plasma on growth of gas sensitivity of SnO₂ films were studied. The plasma treatment of SnO₂ films, obtained by the sol-gel technique, does not alter their phase composition, and gas sensitivity growth does not depend on the type of plasma. Treatment by O-plasma of films prepared by magnetron sputtering, leads to a more significant increase in gas sensitivity than by H-plasma, due to the oxidation of SnO_x film.
9. The phenomena of self-organization of matter in SnO_x layers were identified, consisting in the intensive formation of SnO₂ crystallites with sizes of 4 nm in the process of film deposition by magnetron sputtering (pressure in the Ar-O₂ mixture is 2.7 Pa), and SnO₂ crystallites with sizes of 3 nm at the deposition of films by the sol-gel technique (concentration of Sn 0.14 mol/L in a solution).

5. Acknowledgement

The authors are very grateful to Dmitriyeva E.A. for preparation of the films and Mit' K.A. for AFM measurements.

6. References

- Aboaf, J.A., Marcotte, V.C., Chou, N.J. (1973). Doping of tin oxide films and analysis of oxygen content. *J. Electrochem. Soc.*, Vol. 120, p. 701.
- Adamyan, A.Z., Adamyan, Z.N., Arotyunyan, V.M. (2006). Zol'-gel' tehnologiya polucheniya chuvstvitel'nykh k vodorodu tonkikh plenok (Sol-gel technology for producing hydrogen sensitive thin films). *Al'ternativnaya energetika i ekologiya (Alternative Energy and Ecology)*, Vol. 40, №8, pp. 50–55. In Russian.
- Andryeeva, Ye.V., Zilberman, A.B., Il'in, Yu.L., Makhin, A.V., Moshnikov, V.A., Yaskov, D.A. (1993). Vliyanie etanola na elektrofizicheskie svoïstva dioksida olova (Effect of ethanol on the electrophysical properties of tin dioxide). *Fizika i tehnika poluprovodnikov*, T. 27, №7, pp. 1095–1100. In Russian.
- Anishchik, V.M., Konyushko, L.I., Yarmolovich, V.A., Gobachevskiy, D.A., Gerasimova, T.G. (1995). Struktura i svoïstva plenok dioksida olova (Structure and properties of tin dioxide films). *Nyeorganicheskie materialy (Inorganic Materials)*, Vol. 31, №3, pp. 337–341. In Russian.
- Aranowich, J., Ortiz, A., Bube, R.H. (1979). Thin oxide films prepared by spray hydrolysis. *J. Vacuum Sci. Technol.*, Vol. 16, pp. 994.
- Asakuma N., Fukui T., Toki M., Imai H. (2003) Low-Temperature synthesis of ITO thin films using an ultraviolet laser for conductive coating on organic polymer substrates. *Journal of Sol-Gel Science and Technology*, Vol. 27, pp. 91–95.
- Bakin, A.S., Bestaev, M.V., Dimitrov, D.Tz., Moshnikov, V.A., Tairov, Yu.M. (1997). SnO₂ based gas sensitive sensor. *Thin Solid Films*, Vol. 296, pp. 168–171.
- Bestaev, M. V., Dimitrov, D.Ts., Il'in, A.Yu., Moshnikov, V.A., Träger, F., Steitz, F. (1998). Study of the surface structure of tin dioxide layers for gas sensors by atomic-force microscopy. *Semiconductors*, Vol. 32, iss. 6, pp. 587–589.
- Bosnell, J.R. and Waghorne, R. (1973). The method of growths tin films. *Thin Solid Films*, Vol. 15, pp. 141.
- Brito G.E.S., Ribeiro S.J.L., Briois V., Dexpert-Ghys J., Santilli C.V., Pulcinelli S.H. (1997). Short range order evolution in the preparation of SnO₂ based materials. *Journal of Sol-Gel Science and Technology*, Vol.8, pp. 261–268.
- Buturlin, A.I., Gabuzyan, T.A., Golovanov, N.A., Baranenko, I.V., Yevdokimov, A.V., Murshudli, M.N., Fadin, V.G., Chistyakov, Yu.D. (1983a). Gazochuvstvitel'nye datchiki na osnove metallookisnykh poluprovodnikov (Gas-sensitive sensors based on metal oxide semiconductors). *Zarubezhnaya elektronnaya tehnika*. 10, 269, pp. 3–39. In Russian.
- Buturlin, A.I., Obrezkova, M.V., Gabuzyan, T.A., Fadin, V.G., Chistyakov, Yu.D. (1983b). Elektronnye datchiki dlya kontrolya kontsentratsii etanola v vydykhaemom vozdukh (Electronic sensors for monitoring the concentration of ethanol in the exhaled air). *Zarubezhnaya elektronnaya tehnika*, № 11, pp.67–87. In Russian.

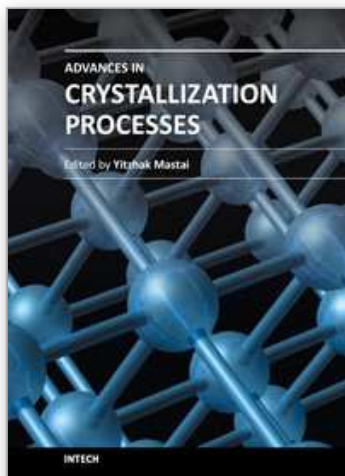
- Chatelon J.P., Terrier C., Roger J.A. (1997). Consequence of the pulling solution ageing on the properties of tin oxide layers elaborated by the sol-gel dip-coating technique. *Journal of Sol-Gel Science and Technology*, Vol. 10, pp. 185–192.
- Das, Debajyoti and Banerjee, Ratnabali (1987). Properties of electron-beam-evaporated tin oxide films. *Thin Solid Films*. Vol. 147. pp.321–331.
- Dibbern, U., Kuersten, G., Willich, P. (1986). Gas sensitivity, sputter conditions stoichiometry of pure tin oxide layers. *Proc. 2nd Int. Meeting on Chem. Sensors. Bordeaux, 1986.* p. 142.
- Dimitrov, D.Ts., Luchinin, V.V., Moshnikov, V.A., Panov, M.V. (1999). Ellipsometry as a rapid method of establishing a correlation between the porosity and the gas sensitivity of tin dioxide layers. *Technical Physics*, Vol. 44, iss. 4, pp.468–469.
- Evdokimov, A.V., Murshudlu, M.N., Podlepetsky, B.I., Rzhhanov, A.E., Fomenko, S.V., Filippov, V.I., Yakimov S.S. (1983). Mikroelektronnye datchiki himicheskogo sostava gasa (Microelectronic sensors of the gas chemical composition). *Zarubezhnaya elektronnaya tehnika*, № 10, pp. 3–39. In Russian.
- Fantini, M., Torriani, I. (1986). The compositional and structural properties of sprayed SnO₂:F thin films. *Thin Solid Films*, Vol. 138, pp. 255–265.
- Geoffroy C., Campet G., Portier J. (1991). Preparation and characterization of fluorinated indium tin oxide films prepared by R.F. sputtering. *Thin Solid Films*, Vol. 202, pp. 77–82.
- Jarzebski, Z.M. (1982). Preparation and physical properties of transparent conducting oxide films. *Phys. Stat. Sol.*, Vol. 71 (a), pp.13–41.
- Jarzebski, Z.M., and Marton, J.P. (1976). Physical properties of SnO₂. *Materials. J. of the Electrochemical Society*. Vol. 123, № 7. pp. 199C–205C; № 9. pp. 299C–310C; № 10, pp. 333C–346C.
- Jiang, J.C., Lian, K., Meletis, E.I. (2002). Influence of oxygen plasma treatment on the microstructure of SnO_x thin films. *Thin Solid Films*, Vol.411, pp. 203–210.
- Jitianu, A., Altindag,Y., Zaharescu, M., Wark, M. (2003). New SnO₂ nanoclusters obtained by sol-gel route, structural characterization and their gas sensing applications. *Journal of Sol-Gel Science and Technology*, Vol. 26, pp. 483–488.
- Karapatnitski, I.A., Mit', K.A., Mukhamedshina, D.M., Baikov, G.G. (2000). Effect of hydrogen plasma processing on the structure and properties of tin oxide thin film produced by magnetron sputtering. *Proc. of the 4th Int. Conf. on Thin Film Physics and Applications*, 8-11 May, 2000. Shanghai, China. Vol. 4086, p. 323.
- Kaur, M., Aswal, D.K., Yakhmi J.V. (2007). Chemiresistor gas sensor: materials, mechanisms and fabrication. In: *Science and Technology of Chemiresistor Gas Sensors*. Editors: Aswal D.K., Gupta S.K. Chapter 2, pp. 33–93.
- Kern, W., Ban, V.S. (1978). In: *Thin Film Processes*. New-York: Academic Press. Ed. J.L. Vossen and W. Kern. P. 257–331.
- Khol'kin, A.I., Patrusheva, T.N. (2006) Ekstraktsionno-piroliticheskiy metod: Poluchenie funktsional'nykh oksidnykh materialov. (Extraction-pyrolytic method: Preparation of functional oxide materials) – M.: Kom Kniga, 288 s. In Russian.
- Kim, K.H., Chun, J.S. (1986). X-ray studies of SnO₂ prepared by chemical vapour deposition. *Thin Solid Films*, Vol. 141, pp. 287–295.

- Kissin V. V., Sysoev V. V., Voroshilov S. A. (1999). Discrimination of acetone and ammonia vapour using an array of thin-film sensors of the same type. *Technical Physics Letters*, V. 25, Iss.8, pp. 657-659.
- Kissin, V. V., Sysoev, V. V., Voroshilov, S. A., Simakov, V. V. (2000). Effect of oxygen adsorption on the conductivity of thin SnO₂ films. *Semiconductors*, Vol. 34, № 3, pp. 308-311.
- Knunians, I.L. (1964). In: *Kratkaya khimicheskaya entsiklopediya* (Brief Chemical Encyclopedia). Moscow: Sovetskaya entsiklopediya, 1964. 1112 p. with illustrations. In Russian.
- Kobayashi, N. (2005). In: *Vvedenie v nanotekhnologiyu* (Introduction to Nanotechnology). Moscow: Binom, Laboratoriya Znaniy, 134 p. In Russian (translated from Japanese).
- Kukuev, V.I., Popov, G.P. (1989). Povyshenie nadezhnosti plenochnykh nagrevatel'nykh elementov na osnove dvoukisi olova (Improving the reliability of film heating elements based on tin dioxide). *Elektronnaya promyshlennost' (Electron industry)*, №3, pp. 33-35.
- Lewin, R., Howson, R.P., Bishop, C.A., Ridge, M.I. (1986). Transparent conducting oxides of metals and alloys made by reactive magnetron sputtering from elemental targets. *Vacuum*, Vol. 36, pp. 95-98.
- Martin, P.J., Netterfield, R.P. (1986). Properties of indium tin oxide films prepared by ion-assisted deposition. *Thin Solid Films*, Vol. 137, pp. 207-214.
- McDonagh, C., Bowe, P., Mongey, K., MacCraith, B.D. (2002). Characterization of porosity and sensor response times of sol-gel-derived thin films for oxygen sensor applications. *Journal of Non-Crystalline Solids*, Vol. 306, pp. 138-148.
- Melsheimer, J., Teshe, B. (1986). Electron microscopy studies of sprayed thin tin dioxide films. *Thin Solid Films*, Vol. 138, pp. 71-78.
- Minami, T., Sato, H., Nanto, H., Takata, S. (1989). Heat treatment in hydrogen gas and plasma for transparent conducting oxide films such as ZnO, SnO₂ and indium tin oxide. *Thin Solid Films*, Vol. 176, pp. 277-282.
- Mishra, S., Ghanshyam, C., Ram, N., Singh, S., Bajpai, R.P., Bedi, R.K. (2002). Alcohol sensing of tin oxide thin film prepared by sol-gel process. *Bull. Mater. Sci.*, Vol. 25, № 3, pp. 231-234.
- Nagamoto Takao, Maruta Yukihiro, Omoto Osami (1990). Electrical and optical properties of vacuum-evaporated indium-tin oxide films with high electron mobility. *Thin Solid Films*, Vol. 193/194, pp. 704-711.
- Okunara, T., Kasai, A., Hayakova, N., Voned, G., Misono, M. (1983). Catalysis by eteropolicompounds. *Journal of catalysis*, Vol. 83, pp. 121-130.
- Ramamoorthy, R., Kennedy, M.K., Nienhaus, H., Lorke, A., Kruis, F.E., Fissan, H. (2003). Surface oxidation of monodisperse SnO_x nanoparticles. *Sensors and Actuators B*, Vol. 88, pp. 281-285.
- Rembeza, S. I. , Svistova, T. V., Rembeza, E. S., Borsyakova, O. I. (2001). The microstructure and physical properties of thin SnO₂ films. *Semiconductors*, Vol. 35, № 7, pp. 762-765.
- Rumyantseva, M.N., Bulova, M.N., Charyeev, D.A., Ryabova, L.I., Akimov, B.A., Arhangel'skiĭ, I.V., Gas'kov, A.M. (2001). Sintez i issledovanie nanokompozitov na osnove poluprovodnikovyykh oksidov SnO₂ i WO₃ (Synthesis and study of

- nanocomposites based on semiconducting oxides, SnO₂ and WO₃). Vestn. Mosk. Un-ta. Ser.2: Khimiya, T. 42, №5, pp. 348–355. In Russian.
- Rumyantseva, M.N., Makyeeva, Ye.A., Gas'kov, A.M. (2008). Vliyanie mikrostruktury poluprovodnikovyykh sensorykh materialov na khemosorbtsiyu kisloroda na ikh poverhnosti (Influence of microstructure of semiconductor sensor materials on chemisorptions of oxygen on their surface). Ros. khim. zhurn. (Zh. Ros. Khim. obva im. D.I.Mendelyeeva) (Ros. Chem. Journal) – Vol. LII, №2, pp. 122–129. In Russian.
- Rumyantseva, M.N., Safonova, O.V., Bulova, M.N., Ryabova, L.I., Gas'kova, A.M. (2003). Gazochuvstvitel'nye materialy na osnove dioksida olova (Gas-sensitive materials based on tin dioxide). Sensor, № 2(8), pp. 8–33. In Russian.
- Rumyantseva, M.N., Safonova, O.V., Bulova, M.N., Ryabova, L.I., Gas'kova, A.M. (2003). Legiruyushchie primesi v nanokristallicheskom diokside olova (Dopants in nanocrystalline tin dioxide). Izvestiya Akademii nauk. Seriya khimicheskaya (Proceedings of the Academy of Sciences. Chemical Bulletin), №6, pp. 1151–1171.
- Ryabtsev, S.V., Yukish, A.V., Khango, S.I., Yurakov, Yu.A., Shaposhnik, A.V.; Domashevskaya, E.P. (2008). Kinetics of resistive response of SnO_{2-x} thin films in gas environment. Semiconductors, vol. 42, issue 4, pp. 481–485.
- Ryzhikov, A.S., Vasiliev, R.B., Rumyantseva, M.N., Ryabova, L.I., Dosovitsky, G.A., Gilmutdinov, A.M., Kozlovsky, V.F., Gaskov, A.M. (2002). Microstructure and electrophysical properties of SnO₂, ZnO and In₂O₃ nanocrystalline films prepared by reactive magnetron. Materials Science and Engineering. B, Vol. 96, pp. 268–274.
- Sanz Maudes, J., Rodriguez, T. (1980). Pyrolysis method for preparing of transparent conducting films. Thin Solid Films, Vol. 69, p. 183.
- Semancik S., Cavicchi R.E. (1991). The growth of thin, epitaxial SnO₂ films for gas sensing applications. Thin Solid Films, Vol. 206, pp. 81–87.
- Seok-Kyun Song. (1999). Characteristics of SnO_x films deposited by reactive ion-assisted deposition. Phys. Rev., Vol. 60, pp. 11137–11148.
- Shanthi, E., Dutta, V., Banerjee, A., Chopra, K.L. (1981). SnO₂ Based Gas Sensitive Sensor. J. Appl. Phys., Vol. 51, pp. 6243–6249.
- Srivastava, R., Dwivedi, R., Srivastava, S.K. (1998a). Effect of oxygen, nitrogen and hydrogen plasma processing on palladium doped tin oxide thick film gas sensors. Physics of Semiconductor Devices. – India, New Delhi: Narosa Publishing House, pp. 526–528.
- Srivastava, R., Dwivedi, R., Srivastava, S.K. (1998b). Effect of oxygen and hydrogen plasma treatment on the room temperature sensitivity of SnO₂ gas sensors. Microelectronics Journal, Vol. 29, pp. 833–838.
- Stjerna B. and Granqvist C.G. (1990). Optical and electrical properties of SnO_x thin films made by reactive R.F. magnetron sputtering. Thin Solid Films, 193/194, pp. 704–711.
- Suikovskaya, N.V. (1971). Khimicheskie metody polucheniya tonkikh prozrachnykh plenok (Chemical methods of thin transparent films). – Leningrad. Khimiya (Chemistry), 200 s. In Russian.
- Suzdalev, I.P. (2006). In: Nanotekhnologiya: fiziko-khimiya nanoklastero, nanostruktur i nanomaterialov (Nanotechnology: physics and chemistry of nanoclusters, nanostructures and nanomaterials), M.: KomKniga, 592 p. In Russian.

- Torkhov, D.S., Burukhin, A.A., Churagulov, B.R., Rumyantseva, M.N., Maksimov, V.D. (2003). Hydrothermal synthesis of nanocrystalline SnO_2 for gas sensors. *Inorganic Materials*. Vol. 39, № 11, pp. 1158-1162.
- Vigleb, G. (1989). In: *Datchiki (Sensors)*. - Moscow: Mir, 196 p. In Russian.
- Watson, J., Ihokura, K. and Coles, S. (1993). The tin dioxide gas sensor. *Meas. Sci. Technol.*, Vol. 4, pp. 713-719.
- Weigtens, C.H.L., Loon, P.A.C. (1991). Influence of annealing on the optical properties of indium tin oxide. *Thin Solid Films, Electronics and Optics*, Vol. 196, pp. 17-25.
- Xu, Ch., Jun, T., Norio, M., Nobory, Y. (1991). Grain size effects on gas sensitivity of porous SnO_2 based elements. *Sensors and Actuators B.*, Vol. 3, pp. 147-155.
- Zang, G. and Liu, M. (1999). Preparation of nanostructured tin oxide using a sol-gel process based on tin tetrachloride and ethylene glycol. *Journal of Material Science*, Vol. 34, pp. 3213-3219.

IntechOpen



Advances in Crystallization Processes

Edited by Dr. Yitzhak Mastai

ISBN 978-953-51-0581-7

Hard cover, 648 pages

Publisher InTech

Published online 27, April, 2012

Published in print edition April, 2012

Crystallization is used at some stage in nearly all process industries as a method of production, purification or recovery of solid materials. In recent years, a number of new applications have also come to rely on crystallization processes such as the crystallization of nano and amorphous materials. The articles for this book have been contributed by the most respected researchers in this area and cover the frontier areas of research and developments in crystallization processes. Divided into five parts this book provides the latest research developments in many aspects of crystallization including: chiral crystallization, crystallization of nanomaterials and the crystallization of amorphous and glassy materials. This book is of interest to both fundamental research and also to practicing scientists and will prove invaluable to all chemical engineers and industrial chemists in the process industries as well as crystallization workers and students in industry and academia.

How to reference

In order to correctly reference this scholarly work, feel free to copy and paste the following:

Daniya M. Mukhamedshina and Nurzhan B. Beisenkhanov (2012). Influence of Crystallization on the Properties of SnO₂ Thin Films, *Advances in Crystallization Processes*, Dr. Yitzhak Mastai (Ed.), ISBN: 978-953-51-0581-7, InTech, Available from: <http://www.intechopen.com/books/advances-in-crystallization-processes/influence-of-crystallization-on-the-properties-of-sno2-thin-films>

INTECH
open science | open minds

InTech Europe

University Campus STeP Ri
Slavka Krautzeka 83/A
51000 Rijeka, Croatia
Phone: +385 (51) 770 447
Fax: +385 (51) 686 166
www.intechopen.com

InTech China

Unit 405, Office Block, Hotel Equatorial Shanghai
No.65, Yan An Road (West), Shanghai, 200040, China
中国上海市延安西路65号上海国际贵都大饭店办公楼405单元
Phone: +86-21-62489820
Fax: +86-21-62489821

© 2012 The Author(s). Licensee IntechOpen. This is an open access article distributed under the terms of the [Creative Commons Attribution 3.0 License](https://creativecommons.org/licenses/by/3.0/), which permits unrestricted use, distribution, and reproduction in any medium, provided the original work is properly cited.

IntechOpen

IntechOpen